EAGE

WORKSHOP
Urban Geophysics

Sunday 4 September 2016

Beatriz Benjumea (Institut Cartogràfic
i Geològic de Catalunya)
Juan José Galiana-Merino (Universidad de Alicante, Dpto.
Física, Ingeniería de Sistemas y Teoría de la Señal)

22nd
EUROPEAN MEETING OF
**ENVIRONMENTAL
AND ENGINEERING
GEOPHYSICS**

SECOND
APPLIED SHALLOW
**MARINE
GEOPHYSICS
CONFERENCE**

FIRST
CONFERENCE ON
**GEOPHYSICS
FOR MINERAL
EXPLORATION
AND MINING**

NEAR SURFACE GEOSCIENCE

4-8 September 2016, Barcelona, Spain

Urban Geophysics

4 September 2016
Barcelona, Spain

Workshop Programme

9:30-9:40   Introduction

9:40-10:25   The Combination of CMP-refraction Seismics with Reflection Seismics to Image Shallow and Deep Structures in Urban Areas
D. Orlowsky (DMT-GmbH & Co. KG)

10:25-11:10   DCIP Tomography for Site Investigation in Urban Areas - New Approaches to Enhance Data Quality and Speed of Data Acquisition
T. Dahlin (Lund University)

11:10-11:25   Coffee Break

11:25-12:10   Development and Applications of a Mems-based Seismic Landstreamer and a Boat-towed Radio-magnetotelluric System – Tackling the Urban Environment
A. Malehmir (Uppsala University)

12:10-12:55   Four Geophones for Seven Possible Objective Functions - Active and Passive Seismics for Tricky Areas
G. dal Moro (Academy of Sciences of the Czech Republic)

12:55-15:00   Lunch

15:00-15:45   Some Limitations of Geophysical Measurements in Urban Environment
C. Cornou (Institut des Sciences de la Terre (ISTerre), IRD, IFSTTAR, CNRS, Université de Grenoble I)

15:45-16:30   Seismic Microzonation of El Ejido Town (SE Spain) from Ambient Noise Measurements
H. Seivane (Universidad de Almería)

16:30-16:45   Coffee Break

16:45-17:30   Seismic Interferometry for Near-surface Applications
E. Galetti (University of Edinburgh)

17:30-18:15   Optimization of Equipment for Ambient Noise Array Measurements
J.J. Galiana-Merino (Universidad de Alicante)

The Combination of CMP-refraction Seismics with Reflection Seismics to Image Shallow and Deep Structures in Urban Areas

D. Orlowsky (DMT-GmbH & Co. KG)

Summary

Seismic techniques image either the deeper underground (P-wave reflection seismic techniques) starting with depths of several tens of meters or they allow to image very shallow structures, down to about 10-20 m (refraction seismics, analyses of surface waves, etc.), only. Often there is a gap in the depth range between the results of reflection seismics and applications which study the near surface underground. Especially in urban areas, where often complex construction projects are planned, detailed information about shallow as well as about deeper structures are needed. In an urban environment seismic data quality is generally decreased and can rapidly vary from one shot location to the other, due to the changing noise conditions. To image the stratigraphy of the complete depth range, starting from the earth's surface down to greater depths in "one" seismic section the results of reflection seismic data processing are combined with images generated with the CMP-refraction seismic technique. Whereas the reflected wave field describe the deeper regions of the underground, the refracted wave field is more related to the shallow parts.

Introduction

In urban areas the investigation of deep structures down to more than several hundred meters combined with a description of shallow underground conditions shows high requirements on data acquisition techniques as well as on processing and interpretation procedures. Seismic techniques usually describe either the deeper underground (P-wave reflection seismic techniques) starting with depths of several tens of meters or they allow to image very shallow structures, down to about 10-20 m (refraction seismic, analyses of surface waves, etc.), only. Often, there is a gap in the depth range between the results of reflection seismics and applications which study the near surface underground. Therefore, the joint interpretation of the various findings can be very challenging. Furthermore, seismic data quality recorded in urban areas is reduced, due to the noisy environment (traffic, construction sites, people walking, etc.) as well as due to the surface conditions (pavement, old fundaments and other anthropogenic effects). A method which increases the signal to noise ratio of refracted waves and which allows to close the gap between the results of reflection seismics and refraction seismics is the Common Midpoint- (CMP-) refraction seismic technique (Gebrande, 1986, Orlowsky *et al.* 1998). With this method the shallow underground can be displayed using the whole information of the "refracted wave field". For applying the CMP-refraction seismic method the same data basis as for reflection seismic data processing can be used. The resulting image represents a so called "intercept time section" to display shallow refractors. This section is transformed into a zero-offset section, well known as a result of reflection seismic data processing. However, this "shallow zero-offset section" is generated on the basis of the refracted wave field describing the shallow parts of the underground. Thus, together with the reflection seismic results, the stratigraphy of the complete depth range, starting from the earth's surface down to greater depths, can be interpreted and disturbances such as faults, weak zones and clefts are located vertically and horizontally.

Seismic data acquisition in urban areas

The characteristic features of an urban environment (buildings, transport infrastructure, underground utilities, vegetation, human life, public interests, etc.) have significant impact on the acquisition as well as on the analysis of seismic data (Bhokonok *et al*., 2006). Hence, extra thoughts need to be put into the design of seismic surveys performed in an urban environment. Figure 1 displays the circumstances under which reflection seismic data acquisition sometimes need to be acquired. Source point locations as well as receiver stations are limited to the road network of the city. In such an environment data quality can change rapidly from one shot position to the next one.

Figure 1 *Acquisition of seismic data in an urban environment. Vibroseis trucks are generating seismic signals usually for reflection seismic data processing and interpretation, only.*

Figure 2 displays examples of seismic raw data recorded along profiles in an urban area. It can clearly be recognised, that the data characteristics differ from one shot location to the other. Whereas, **Figure 2a** displays nearly undisturbed data, the signal to noise ratio in **Figure 2b** is decreased due to the traffic along the profile. The refracted waves displayed in **Figure 2c** are superimposed by high frequency first break phases belonging to signals which are mainly guided within the road pavement. Thus, signal processing need to be adjusted in order to increase the signal to noise ratio and to suppress the first breaks guided within the road pavement. Furthermore, some repetitions of the source signal can be recognised, especially at times of about 230 ms and 300 ms. These repetitions are due to a bouncing effect of the seismic source on the strong pavement.
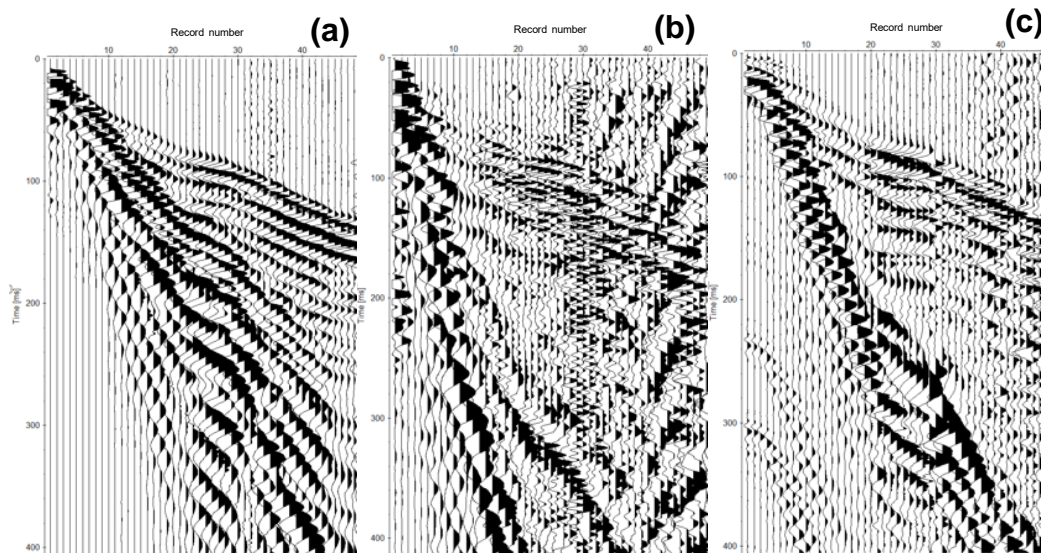

Figure 2 Examples of the raw data (trace normalized) recorded along profiles in an urban area. (a) Undisturbed data. (b) Noisy data. (c) Data collected with the source position on strong pavement.

Combination of CMP-refraction seismics with reflection seismics

To image the stratigraphy of the complete depth range, starting from the earth's surface down to greater depths in "one" seismic section the results of reflection seismic data processing are combined with the images generated with the CMP-refraction seismic technique. Whereas the reflected wave field describe the deeper regions of the underground, the refracted wave field is more related to the shallow parts. For data processing the same data basis is used for both, reflection seismics and CMP-refraction seismics. In a first step standard reflection seismic data processing is performed resulting into a stacked zero-offset time section. For an optimized CMP-refraction seismic procedure the results of the General Reciprocal Method (GRM, Palmer 1990) are needed (Orlowsky et. al, 1998). The combination of CMP-refraction seismics with the GRM generates a so called intercept time section which is subsequently converted into a zero-offset time section of the refracted wave field. To generate a zero-offset section out of the refracted and reflected wave fields the following processing procedure is applied:

1. Data input into the processing system.
2. Edit of bad traces and geometry input (X, Y, Z-coordinates for traces and shot locations).
3. Standard reflection seismic data processing
4. Band-pass filtering of the refracted wave field to suppress the high frequency waves guided in pavements.
5. Determination of the first arrival times of the refracted waves and generation of travel-time fields.
6. Inversion of the travel-time fields applying the GRM, generation of a velocity model and determination of the optimum XY-values (XY_{opt}) for different refractors.

7. CMP-offset-sorting of the wave field (U^{CMP}) and partial RADON-transformation (V_j^{CMP}) at each CMP to generate the intercept time sections for each refractor (j) after the following equation (Orlowsky et. al., 1998):

$$V_j^{CMP}(p_j^{CMP}, \tau^{CMP}) = V_j^{CMP}(\frac{1}{v_j^{GRM}}, \tau^{CMP}) = \int_{XY_{opt}}^{XY_{opt}+\delta} U^{CMP}(x, \frac{1}{v_j^{GRM}}x + \tau^{CMP})dx$$

8. Determination of intercept times (τ^{CMP}) within the intercept time section.
9. Conversion of the intercept time section into a zero-offset section using intercept times and wave velocities v_j^{GRM} determined with the GRM. The following equation is applied for the conversion (Orlowsky et. al., 1998):

$$t_0^{CMP} = \frac{v_2^{CMP}\tau_2^{CMP}}{\sqrt{(v_2^{CMP})^2 - (v_1^{CMP})^2}}$$

with t_0^{CMP} = Zero-offset reflection times.

10. Merging (weighted stacking) of the zero-offset section of the refracted wave field with the zero-offset section of the reflected wave field.
11. Post-Stack-Depth-Migration of the merged zero-offset section.
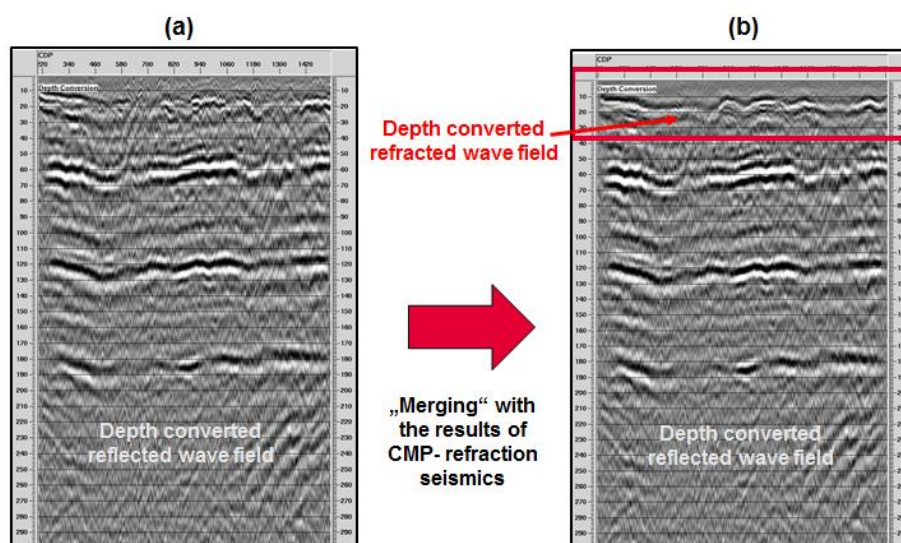
Results of seismic data processing

Figure 3 *Example for results of standard reflection seismic data processing of urban seismic data after depth conversion (**a**) and for a combination of CMP-refraction seismics (red rectangle) with reflection seismics after merging and depth conversion (**b**).*

Figure 3 displays an excerpt of the results of seismic data processing for standard reflection seismic procedures (Figure 3a) and the results for the combination of CMP-refraction seismics with reflection seismics (Figure 3b) of the same data set. The raw data were collected in an urbanized area and should be used for both, deep reflection seismic interpretation as well as for the analysis of the shallow underground. Due to the better signal to noise ratio of the refracted wave field the reflector/refractor down to a depth of about 30 m (red rectangle) becomes much clearer and thus, the depth section of Figure 3b can be better interpreted with respect to both, deep and shallow structures. Therefore, an interpretation of the stratigraphy and tectonic elements for the complete depth range, starting from the earth's surface down to greater depths can be downward continued with information gathered from drillholes.
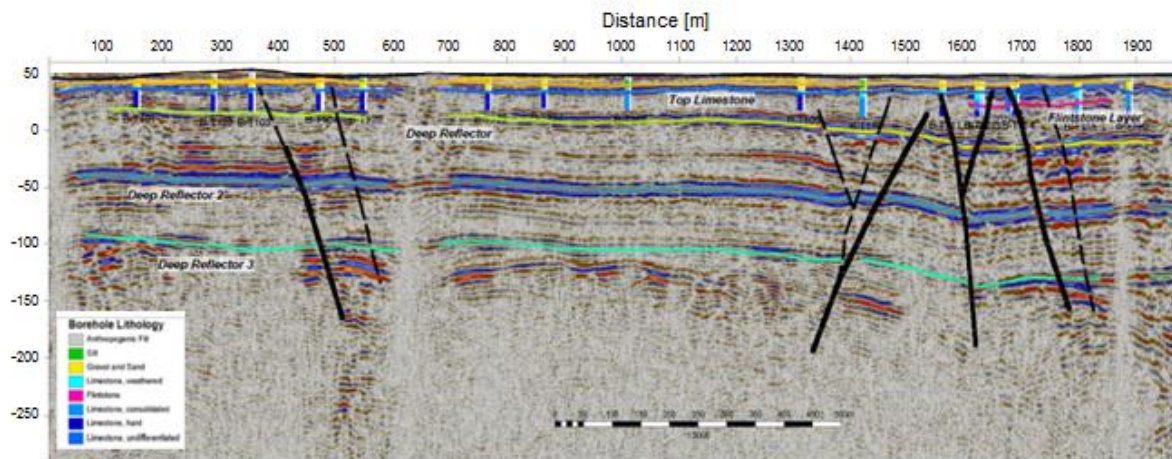
Figure 4 *Joint interpretation of shallow structures dissolved with the results of CMP-refraction seismics (Top Limestone) and drillhole information and deeper elements (Deep Reflectors 1-3) resolved with reflection seismic data processing.*

Figure 4 displays an example for the joint interpretation of shallow structures with the results of CMP-refraction seismics (Top Limestone) and drillhole information as well as deeper elements (Deep Reflectors 1-3) resolved with reflection seismic data processing. Hence, four main layer interfaces are interpreted which show the stratigraphy of the complete depth range, starting from the earth's surface down to a depth of about 300 m (-250 m NN). Disturbances such as faults, weak zones and clefts are located vertically and horizontally. The interpreted elements are verified by the drillings down to the depth of the first Deep Reflector. Especially, the tectonic elements at distances between 1300 m and 1800 m were detected by the drillhole data analysis together with the CMP refraction seismic results.

Conclusions

The combination of CMP-refraction seismics with reflection seismic processing results enables a joint display of the stacked refracted and reflected wave fields in one depth section. This depth section is used for the interpretation of the stratigraphy and tectonic elements of the complete depth range, starting from the earth's surface down to greater depths. With additional information gathered from drillholes this geological model is verified. Furthermore, refractors and reflectors are identified by the drillhole data. These extensive combinations of different processing and analyses techniques are needed especially in urban areas, where data acquisition procedures are much more complex. Data acquisition in an urban environment results into data quality, which generally is decreased and which can rapidly vary from one shot location to the other, due to the changing noise conditions. On the other hand, for complex construction projects detailed information about the complete depth rage from the earth's surface down to several hundred meter is extremely necessary. Therefore, the application of these extensive combinations of processing and analyses techniques are justified.

References

Bhokonok, O., Prado, R., Alcazar, L. [2006] Comparative tests of seismic sources and geophones aiming at shallow reflection seismic investigation in urban areas. *Revista Brasileira de Geofísica*, **24**(1), 81-89.

Gebrande, H. [1986] CMP-Refraktionsseismik. In: *Seismik auf neuen Wegen*, **6**. Mintrop-Seminar, Dresen, L., Fertig, J., Rüter, H., Budach, W. (Eds) Unikontakt, Ruhr-Universität Bochum, 191-206.

Orlowsky, D., Rüter, H. and Dresen, L. [1998] Combination of common-midpoint-refraction seismics with the generalized reciprocal method. *Journal of Applied Geophysics,* **39**, 221-235.

Palmer, D. [1986] Refraction seismics, the lateral resolution of structure and seismic velocity. In: Helbig, K. and Treitel, S. (Eds.) *Handbook of Geophysical Exploration*, **13**. Geophysical Press, London - Amsterdam.

DCIP Tomography for Site Investigation in Urban Areas - New Approaches to Enhance Data Quality and Speed of Data Acquisition

T. Dahlin (Lund University), P.-I. Olson (Lund University), G. Fiandaca (Aarhus University), E. Auken (Aarhus University) & J.J. Larsen (Aarhus University)

Summary

Demand for land for infrastructure, housing, recreation and industry will increase at the same rate as the migration to our cities continues. A solution to handle this would be to increase the use of underground facilities, but this requires first-rate knowledge of structural data, bedrock and soil geology, geotechnical conditions, nearby underground facilities, buried waste, contaminated ground and groundwater. Geoelectrical imaging in the form of Direct Current resistivity and time-domain Induced Polarisation (DCIP) tomography is a tool that can be used to provide such information. DCIP tomography in urban areas can however be demanding due to site characteristics that require a 3D surveying approach, with time consuming data acquisition as a consequence. In order to make the method time and cost efficient the measurement process needs to be speeded up by using multi-channel data acquisition equipment and optimising the measurement sequences, In addition measurement of IP in the on-time with a 100% duty cycle can reduce the measuring time by close to 50%, and at the same time double the signal-to-noise ratio. Data distortions from different noise sources is another problem which can be addressed with a set of signal processing tools that can double the spectral range of the IP data, thus enhancing the possibilities to extract additional material characteristic information. There is, however, noise from the train systems that cannot be handled by this approach but require developments of new noise filtering techniques or measurements when the trains do not operate.

Introduction

Demand for land for infrastructure, housing, recreation and industry will increase at the same rate as the migration to our cities continues. A solution to handle this would be to increase the use of underground facilities for the transportation, garages, warehouses, offices and housing. Planning and development of urban, underground infrastructure must however be based on sustainability. The solutions can be adapted to, deter and resist climate change. Sustainable development requires that energy efficiency is taken into account both during the construction phase and the operation of underground infrastructure.

Unstable rock, groundwater inflow and other unforeseen ground conditions are risk factors that often lead to delays and large additional costs in connection with underground infrastructure construction work. The additional cost is not only economical but also adverse to the environment and climate. Other risk factors include encountering buried waste or contaminated ground as these can pose short term or long term risks for health, environment, construction integrity or economy, or a combination of these. In order to handle these risks first-rate knowledge of structural data, bedrock and soil geology, geotechnical conditions, nearby underground facilities, buried waste, contaminated ground and groundwater is needed.

Geoelectrical imaging in the form of Electrical Resistivity Tomography (ERT) and Direct Current resistivity and time-domain Induced Polarisation (DCIP) tomography is a tool that has been used successfully in such contexts in rural or semi urban areas. The provided information can be used to pinpoint where to place detail investigations such as drilling and sampling so that they are placed in an intelligent way, avoiding to miss key site information and thus decreasing the uncertainties and risks in the subsequent process of planning, construction and operation of underground infrastructures. Applying the technique in urban areas is however more demanding.

DCIP Tomography

Data acquisition for ERT and DCIP tomography is based on transmitting current pulses between pairs of electrodes while at the same time measuring the induced potential via other electrode pairs. Linear electrode spreads are used for 2D data acquisition, whereas 3D data acquisition ca be done by measuring on grids or other layouts of electrodes (e.g. Loke *et al*. 2014; Tejero-Andrade *et al*. 2015) or by adding together data from a number of 2D surveys. Inversion is used to create models of estimated distributions of electrical properties based on the field data, which is done by iteratively adjusting the resistivity, and if included chargeability, of the model cells of a finite difference or finite element model of the ground (e.g. Loke *et al* 2014).

ERT is a well-established technique in site investigation for new infrastructure in rural areas (e.g. Danielsen and Dahlin 2009). The use of ERT in urban areas is however limited by access to placing linear electrode spreads over the area of investigation due to physical obstacles such as buildings, roads, etc. Furthermore, the underground environment can be too complex to be resolved with 2D ERT due to the 3D nature of the environment. This calls for 3D investigation approaches, which however can become very time-consuming due to the large amounts of data required for reliable 3D inversion. It has furthermore been shown that induced polarisation can add significant information in some cases (e.g. Dahlin and Leroux 2012), which makes it desirable to acquire it simultaneously.

Extraction of spectral information in the inversion process of time-domain (TD) induced polarization (IP) data is a way to enhance the TDIP method, by e.g. inverting for the Cole-Cole parameters (Fiandaca *et al*. 2013). Data interpretation is here evolving from a qualitative description of the subsurface, able only to discriminate the presence of contrasts in chargeability parameters, towards a quantitative analysis of the investigated media, which would allow for detailed soil- and rock-type characterization. This, however, puts higher demands on spectral range and quality of the data, and it

can be shown that it is important to use long enough current pulses in order not to lose spectral information and signal-to-noise level (Olsson *et al*. 2015), with associated implications for the time required to measure the data.

Data Acquisition with 100% Duty Cycle Waveform

Combined resistivity and time-domain direct current induced polarization measurements are traditionally carried out with a 50% duty cycle current waveform, taking the resistivity measurements during the on-time and the IP measurements during the off-time. One drawback with this method is that only half of the acquisition time is available for resistivity and IP measurements, respectively, which can lead to very long measurement time if current pulses of several seconds are used in order to resolve the IP characteristics of the subsurface. This limitation can be addressed by using a current injection with 100% duty cycle and taking also the IP measurements in the on-time. With numerical modelling of current waveforms with 50% and 100% duty cycle we have shown that the waveforms have comparable sensitivity for the spectral Cole-Cole parameters and that signal level is increased up to a factor of 2 if the 100% duty cycle waveform is used.

Inversion of field data acquired with both waveforms confirms the modelling results and shows that it is possible to retrieve similar inversion models with either of the waveforms when inverting for the spectral Cole-Cole parameters with the waveform of the injected current included in the forward computations. Consequently, our results show that on-time measurements of IP can reduce the acquisition time by up to 50% and increase the signal-to-noise ratio by up to 100% almost without information loss. Our findings can contribute and have large impact for DCIP surveys in general and especially for surveys where time and reliable data quality are important factors. Specifically, the findings are of value for DCIP surveys conducted in urban areas where anthropogenic noise is an issue and the heterogeneous subsurface demands time-consuming 3D acquisitions.
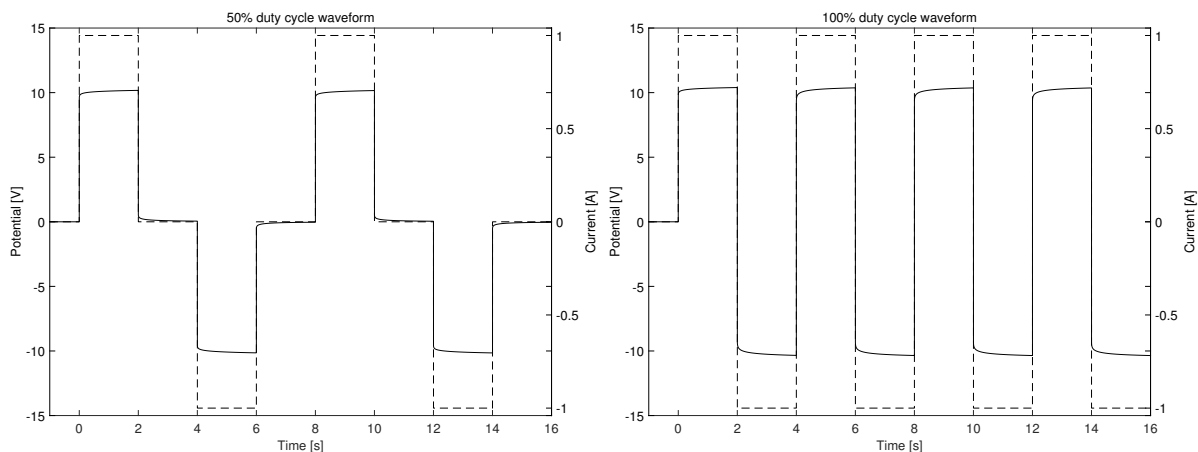

Figure 1 Modelled waveform for the 50% (left) and 100% (right) duty cycle waveform showing measured potential (solid line) and injected current (dashed line). Twice as many stacks are achieved with the 100% duty cycle compared to the 50% duty cycle with the same acquisition time. (Olsson et al. 2015)

Signal Processing

Harmonic electrical noise can be a severe problem when doing DCIP tomography in urban areas. In addition to the regular power grid operating at 50 Hz or 60 Hz, disturbances from industry and train or tram traffic can be present at high levels and be highly variable in time. The established approaches for handling harmonic noise is to use either low pass filtering or data integration over time intervals that are multiples of the period of the base frequency of the power line. This limits the possibility of

extracting early time decay data, especially for sites with noise from train system operating on 16 2/3 Hz or 25 Hz as is the case in many countries.

Recent developments in TDIP acquisition equipment have given access to full waveform recordings of measured potentials and transmitted current, opening a breakthrough for data processing. For measuring at early times, we developed a new method for removing the significant noise from powerlines contained in the data through a model-based approach, localizing the fundamental frequency of the powerline signal in the full-waveform IP recordings (Olsson *et al.* 2016). By this, we cancel both the fundamental signal and its harmonics. The self-potential drift in the measured potentials distort the shape of the late time IP responses. For measuring at late times, we developed an algorithm for removal of the self-potential drift. Usually constant or linear drift-removal algorithms are used, but these algorithms fail in removing the background potentials due to the polarization of the electrodes previously used for current injection. We developed a drift-removal scheme that model the polarization effect and efficiently allows for preserving the shape of the IP responses at late times. Furthermore, a novel and efficient processing scheme for identifying and removing spikes in TDIP data was developed. The noise cancellation and the de-spiking allow the use of earlier and narrower gates, down to a few milliseconds after the current turn-off. In addition, tapered windows are used in the final gating of IP data, allowing the use of wider and overlapping gates for higher noise suppression with reduced signal distortion. Uncertainty estimates are essential in the inversion of IP data. Therefore, in the final step of the data processing, we estimate the data standard deviation based on the data variability within the IP gates and the misfit of the background drift removal.

Overall, the removal of harmonic noise, spikes, self-potential drift, tapered windowing and the uncertainty estimation allows for doubling the usable range of TDIP data to almost four decades in time (see example in Figure 2), which will significantly advance the possibility of extracting spectral information from TDIP data. Even without aiming at spectral inversion of the DCIP data it will enhance the possibilities of extracting good quality resistivity and chargeability data in noisy environments. There is, however, noise from the train systems that cannot be handled with this approach, e.g. metro trains running on DC power supply, but require development of new noise filtering approaches or measurement at night when the train systems do not operate (Dahlin *et al.* 2016).
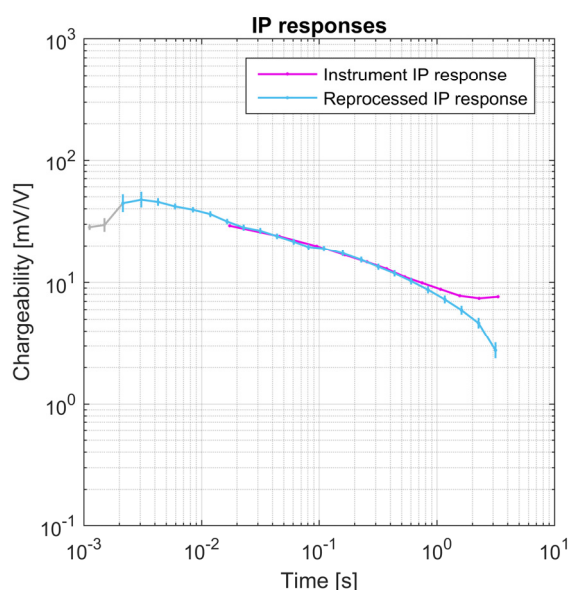

Figure 2 *IP responses from instrument processing (magenta, instrument output) and the redesigned processing scheme (light blue) with error bars corresponding to one STD. Gates rejected by processing for containing spikes are marked in grey. (Olsson et al. 2016)*

Conclusions

DCIP tomography in urban areas can be demanding due to site characteristics that require a 3D surveying approach, with time consuming data acquisition. In order to make the method time and cost efficient the measurement process needs to be speeded up by using multi-channel data acquisition equipment and optimising the measurement sequences, In addition measurement of IP in the on-time with a 100% duty cycle can reduce the measuring time by close to 50%, and at the same time double the signal-to-noise ratio. Data distortions from different noise sources is another problem which can be addressed with a set of signal processing tools that can double the spectral range of the IP data, thus enhancing the possibilities to extract additional material characteristic information. There is, however, noise from the DC powered train systems that cannot be handled by this approach but require developments new noise handling techniques or measurement when the trains do not operate.

Acknowledgements

References

Dahlin T., Wisén R. and Rossi M. [2016] Urban Underwater ERT for Site Investigation in Lake Mälaren, Sweden. *Procs. Near Surface Geoscience 2016*, 4-8 September 2016, Barcelona.

Dahlin T. and Leroux V. [2012] Improvement in time-domain induced polarisation data quality with multi-electrode systems by separating current and potential cables. *Near Surface Geophysics*, **10**, 545-565.

Danielsen B.E. and Dahlin T. [2009] Comparison of geoelectrical imaging and tunnel documentation. *Engineering Geology*, **107**, 118-129.

Fiandaca, G., Ramm, J., Binley, A., Gazoty, A., Christiansen, A.V., Auken, E. [2013] Resolving spectral information from time domain induced polarization data through 2-D inversion. *Geophysical Journal International*, **192**, 631-646.

Loke M.H., Wilkinson P.B., Uhlemann S.S., Chambers J.E. and Oxby L.S. [2014] Computation of optimized arrays for 3-D electrical imaging surveys. *Geophys. J. Int.*, **199**, 1751-1764.

Fiandaca G., Olsson P.-I., Juul Larsen J., Dahlin T. and Auken E. [2016] Doubling the spectrum of time-domain induced polarization by harmonic de-noising, drift/spike removal and tapered gating. *Procs. Near Surface Geoscience 2016*, 4-8 September 2016, Barcelona, Spain.

Olsson P.-I., Dahlin T., Fiandaca G. and Auken E. [2015] Measuring time domain spectral induced polarization in the on-time – decreasing the acquisition time and increasing the signal levels. *Journal of Applied Geophysics*, **123**, 316-321.

Olsson P.-I., Fiandaca G., Dahlin T. and Auken E. [2015] Impact of Time-domain IP Pulse Length on Measured Data and Inverted Models. *Procs. Near Surface Geoscience 2015*, 6-10 September 2015, Torino, Italy,.

Tejero-Andrade A., Cifuentes G., Chávez R.E., López-González A.E. and Delgado-Solórzano C. [2015] L- and CORNER-arrays for 3D electric resistivity tomography: an alternative for geophysical surveys in urban zones, *Near Surface Geophysics*, **13**, 355-367.

Development and Applications of a Mems-based Seismic Landstreamer and a Boat-towed Radio-magnetotelluric System – Tackling the Urban Environment

A. Malehmir (Uppsala University), M. Bastani (Geological Survey of Sweden), B. Brodic (Uppsala University), S. Mehta(Uppsala University), and S. Wang (Uppsala University)

Summary

Urban environment poses by far a different challenge to most geophysical surveys than those of other places. Given the logistic challenges, space limitations, mixed land and water bodies, various types of noise, source and receiver coupling, and urban underground complexities, new and refined ways to better tackle these issues are necessary. In the frame of an industry-academia consortium, we have developed a digital, MEMs-based, 3C seismic landstreamer and a boat-towed radio-magnetotelluric (RMT) system that can partly overcome some of these challenges in the urban environment. We present several case studies of their applications for urban underground infrastructure planning projects. We, for example, illustrate that the seismic streamer is free of electromagnetic noise, allows high-resolution broadband data recording and by far superior to its geophone-type predecessors when it comes to its full spectrum of applications. The boat-towed RMT system combined with additional low-frequency controlled sources make the method quite fast, e.g., 5 km line data per day, and reliable for bedrock mapping and fracture delineation, of which examples will be presented.

Introduction

Urban expansion and hence infrastructures because of the population growth are inevitable. However to reduce the environmental impact and better planning, various geophysical, hydrogeological and geotechnical studies are necessary. All these methods one way or another are challenged in urban environment due to various degrees of complexities imposed by logistics, limited space, noise, geological unknowns, and a mixture of land and water bodies where subsurface characterizations should optimally and cost-effectively be done. Geophysical methods, while non-invasive, are known to have trouble in these types of environments requiring a better way of thinking on how to tackle the issues mentioned above. Successful approaches using streamers for fast data acquisition, ambient noise recording to retrieve shear-wave velocity, and multi-method approaches to overcome individual method's shortcoming have been introduced and shown to be successful. Learning lessons from these approaches, within an academia-industry consortium, we have developed two unique state-of-the-art geophysical acquisition systems for various near-surface applications but particularly geared towards urban environment and for underground infrastructure planning projects. A digital, MEMs-based (micro-electromechanical system) 3C seismic streamer (Figure 1a) was developed that is light, fast to deploy, broadband (0-800 Hz), uses GPS signal for time-sampling and stamping hence can be integrated with autonomous data recorders, and allows several field test possibilities (e.g., tilt and gravity). In addition, RMT system, which uses distant radio-transmitters as EM source, was modified and further upgraded in the project to allow being towed using small boats for subsurface resistivity imaging over lakes, rivers and brackish waters (Figure 1b). Both systems have been used at several sites and for various targets, after many the so-called backyard tests. A detailed description of the two systems can be found in Brodic *et al.* (2015) and Bastani *et al.* (2015), respectively. Our objectives here are to present some technical aspects of the systems and provide example data from them.
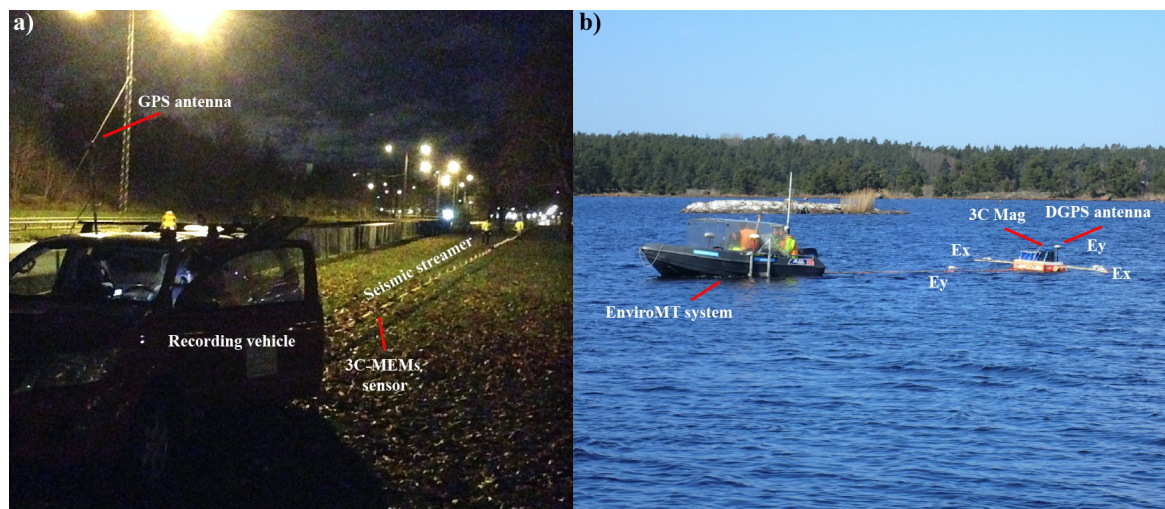

Figure 1 (a) Seismic landstreamer developed in the project as employed in its early stage for site characterization across one of the main planned access ramps of the Stockholm Bypass multi-lane tunnel, and (b) boat-towed RMT system as employed for fracture mapping over the Äspö tunnel.

Seismic landstreamer

The streamer sensors (of DSU3 type) were first tested against plant 10 and 28 Hz geophones and then plant DSU3 sensors in order to check the overall performance of the sensors and the streamer setup. Encouraging results were observed leading to the full development of the streamer. The current streamer setup comprises of 5 segments each containing 20-3C sensors 2-4 m apart giving currently a total length of 240 m that can easily be shortened if required. The streamer was also tested against several vertical- and horizontal-type sources and in more than 10 sites for various infrastructure developments. A recent test conducted inside a tunnel using a combination of the streamer and plant

type geophones for delineating a major fracture system proved the potential of the sensors used in the streamer. Figure 2 shows an example shot gather where the streamer was placed in front of a major fracture system intersecting the tunnel and in the middle of a line where on both sides geophones where planted into the bedrock for the experiment. Streamer data clearly show no contamination of high-voltage and high-amperage electric noise pickup from the power cables running on the side of the tunnel while this is strong on the geophone data. The frequency content of the streamer data is much higher, moreover P-S and S-P conversions from the fracture system are better observed in the streamer data. These demonstrate why digital and broadband sensors more appropriate in urban environment where power cables, trains and trams are abundant everywhere.
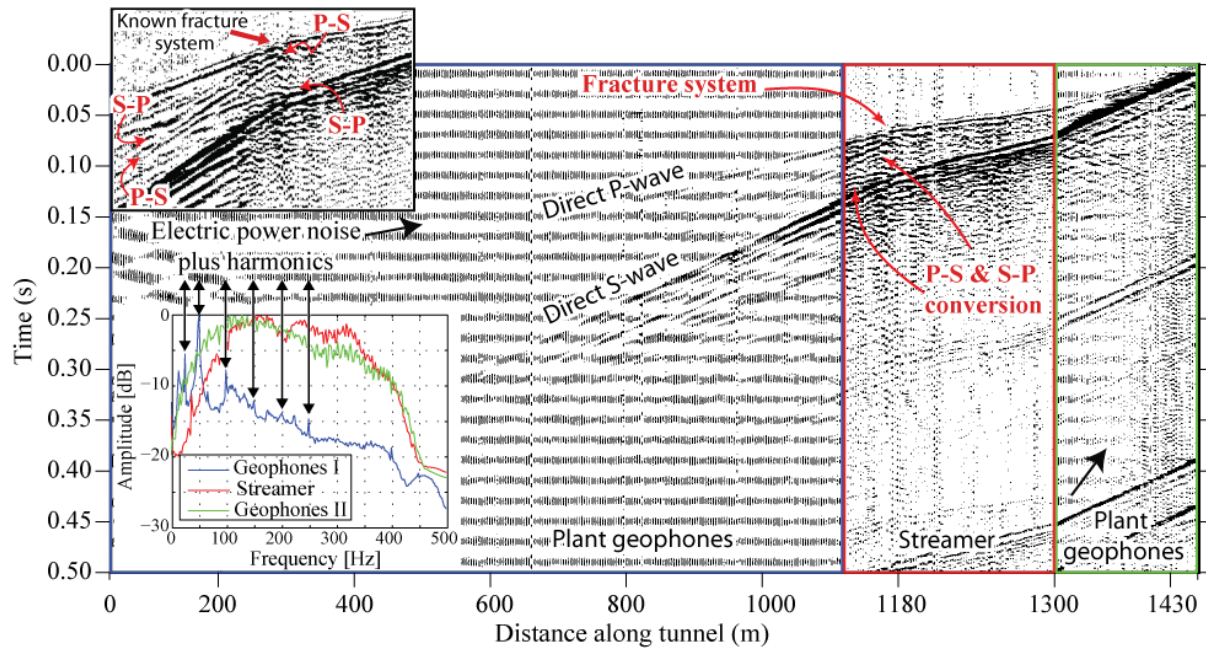

Figure 2 Example shot gather acquired from a tunnel experiment showing the quality of streamer data in comparison with the plant geophones. Note the 50 Hz noise contamination and its harmonic sequence in the geophone data that are totally absent in the streamer data. A major fracture system inside the tunnel was the target of this study producing strong wave-mode conversions (P-S and S-P) that are better noticeable in the streamer data (see the inset on the top).

As an example, the streamer was used for the planning of an underground double-track train tunnel in the city of Varberg in southwest Sweden. Targets were depth to bedrock and weakness zones (e.g., fracture zones) in it. More than 7 km of high-resolution seismic data, 25 profiles, were acquired using 2-4 m source and receiver spacing and an accelerated weight-drop (ESS100) source. At places where placing the streamer was not possible (e.g., at road crossings), wireless recorders were deployed; these data were later merged with the streamer data using the GPS time of the active shots recorded on the streamer data. Details of the data acquisition and results can be found in Malehmir *et al*. (2015). As an example we present first-break tomography results (Figure 3) from the city centre area and their correlations with borehole data (bedrock depth) provided to us for this study. A good correspondence can be observed in most places illustrating the success of the streamer in this project.

Boat-towed RMT

Fresh-water lakes and rivers, as well as brackish water bodies near big cities such as Stockholm cover about 7% of the Swedish land. Geophysical surveys are limited and confined to mainly marine seismic surveys of limited channels and offsets. Some underwater ERT surveys have been carried out however requiring manpower, extensive acquisition setup and detailed planning, which makes their use only optimal for specific target delineations. Pioneered by experts from the Geological Survey of Sweden (Bastani *et al*., 2015), an existing RMT acquisition system developed at Uppsala University

(EnviroMT) was modified to allow data acquisition over lakes and rivers. The system was used, after an initial test close to Uppsala, across three water passages where the planned Stockholm Bypass tunnel crosses. Within 3 days (5 hours per day) more than 15 km of RMT line data were acquired. Data showed excellent quality justifying its inversion in order to obtain resistivity structures of the subsurface. Determinant data were used for this purpose. Inversion results clearly depict water depth, quaternary sediments overlying bedrock, and bedrock level close to the shorelines.
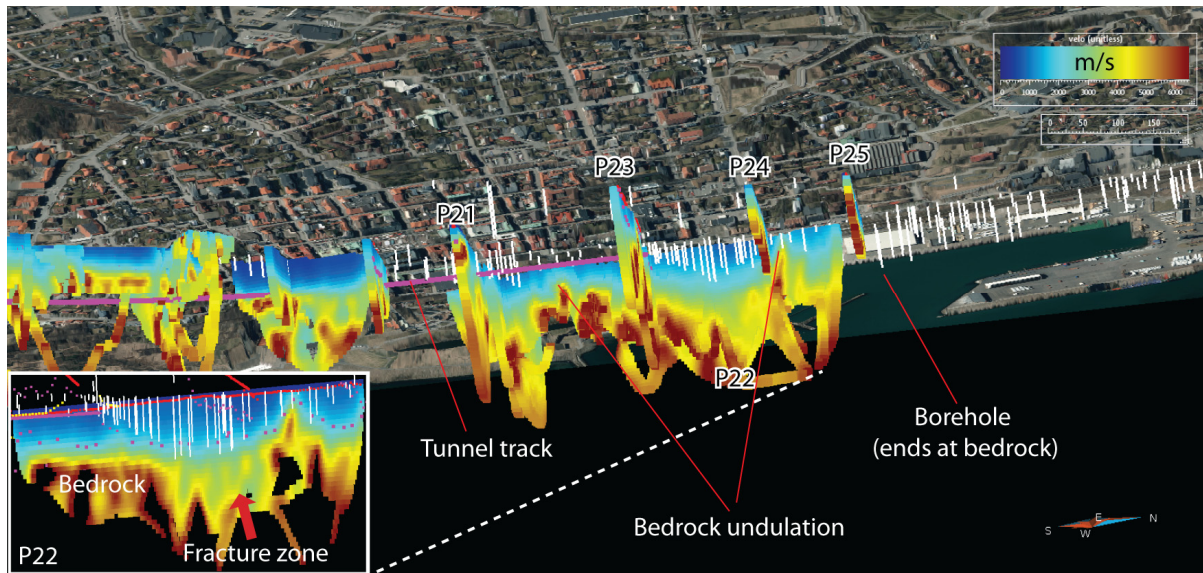

Figure 3 *3D view (from below) showing first-break tomography results in the city centre (about 12 profiles are shown) and available borehole data (until May 2016). The planned tunnel is shown using purple line. A close up of the results along profile 22 is shown as an inset.*

Figure 4 shows a 3D view of the resistivity models from two of the water passages. Interestingly, a major low-resistivity zone is observed in all the water passages that can be either associated with the thickening of the quaternary sediments or presence of weakness zones running along the water passages (or combined). It is today known that there are major faults and fracture systems in these locations filled with conductive materials, highly hydraulically conductive, likely give rise to the low-resistivity zones observed in the RMT data. To provide information from deeper parts, a new experiment was recently conducted (March 2016) where a double horizontal dipole transmitter, controlled remotely from the receiver site, was utilized to transmit EM signals as low as 2.5 KHz. Because of longer data acquisition time (4-5 minutes), the experiment was done during the winter on the frozen lake allowing a better control on the data quality. Excellent data were recorded. These data are currently being analysed and prepared for modelling. Preliminary results will be presented.

Conclusions

Two modern geophysical systems have been developed and employed for various near-surface applications with a particular focus on urban underground infrastructure planning projects. Data acquired by the systems show excellent quality allowing high-resolution imaging of the subsurface structures. While there are rooms for improvements, they are currently being used in several infrastructure-planning projects inside and outside Sweden illustrating their potentials. Future developments will include exploiting the broadband frequency nature of the streamer data and development of a 3C source that can generate broad frequency data that the streamer sensors are capable of recording. Boat-towed RMT system will require new hardware and software developments. A DGPS system was recently linked to the system to provide high-precision geodetic surveying of the acquisition points, which proved to be important for this type of survey.
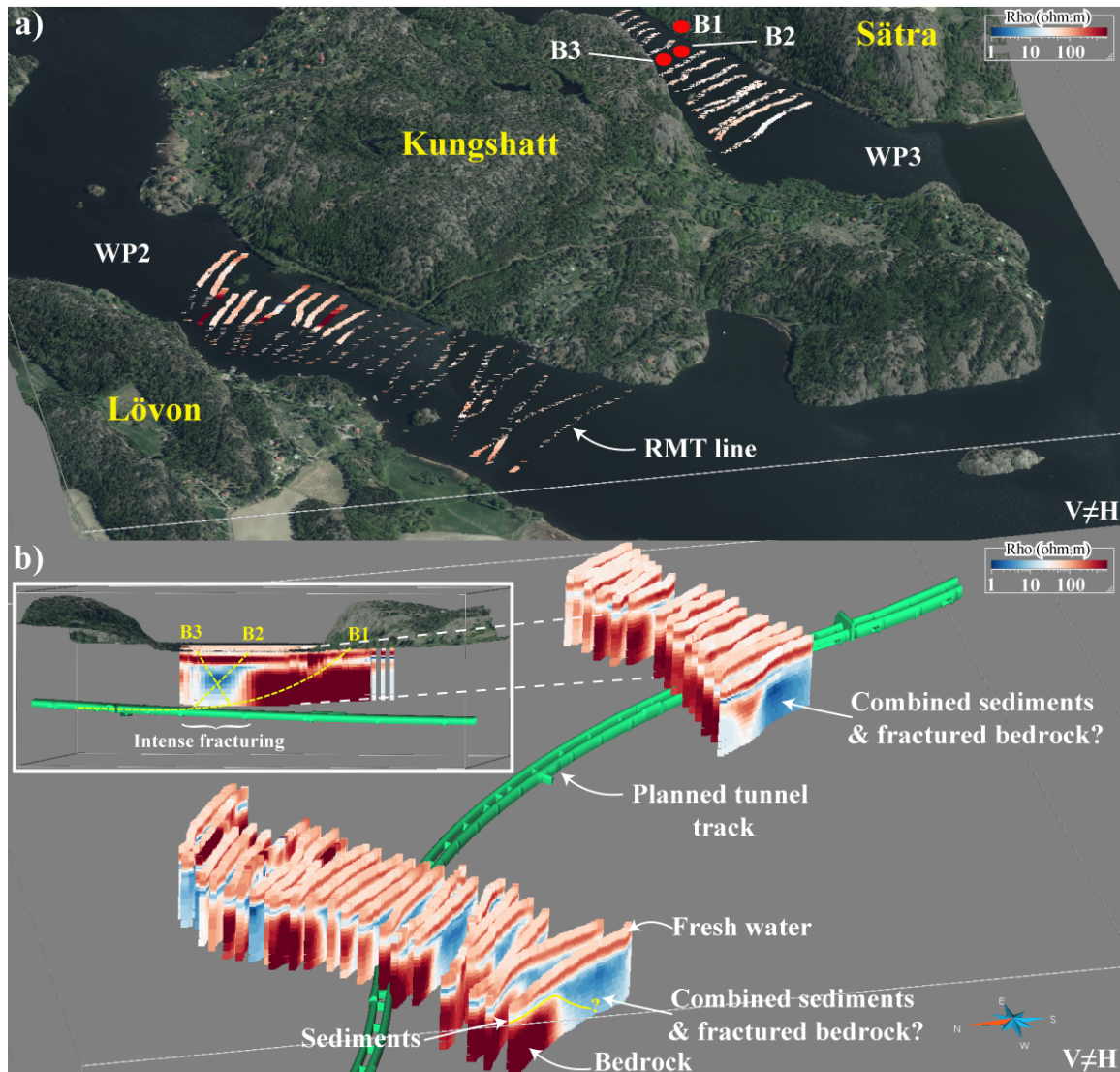
Figure 4 *3D views showing (a) RMT lines from the two of the three water passages where measurements were conducted, and (b) resistivity models and interpretations of features observed. Inset in (b) shows a close of a RMT line, close to the tunnel track, where core data are available.*

Acknowledgments

References

Bastani, M., Persson, L., Mehta, S. and Malehmir, A. [2015] Boat-towed radio-magnetotellurics – A new technique and case study from the city of Stockholm. *Geophysics*, **80**, B193-B202.

Brodic, B., Malehmir, A., Juhlin, C., Dynesius, L., Bastani, M. and Palm, H. [2015] Multicomponent broadband digital-based seismic landstreamer for near surface applications. *Journal of Applied Geophysics*, **123**, 227-241.

Malehmir, A., Zhang, F., Dehgahnnejad, M., Lundberg, E., Döse, C., Friberg, O., Brodic, B., Place, J., Svensson, M. and Möller, H. [2015] Planning of urban underground infrastructure using a broadband seismic landstreamer—Tomography results and uncertainty quantifications from a case study in southwest of Sweden. *Geophysics*, **80**, B177-B192.

Four Geophones for Seven Possible Objective Functions - Active and Passive Seismics for Tricky Areas

G. Dal Moro (Academy of Sciences of the Czech Republic)

Summary

Through an urban case study, we illustrate the holistic analysis of seven components related to surface-wave propagation as defined by both active and passive acquisition procedures.

All the considered components are obtained through the exploitation of the data recorded by only four sensors (three vertical-component and one 3-component geophones).

Regarding the passive datasets, in addition to the conventional HVSR (*Horizontal-to-Vertical Spectral Ratio*), we also consider the Rayleigh-wave dispersion defined through the *Miniature Array Analysis of Microtremors* (MAAM) which, differently than other passive multi-channel methodologies, requires a very limited room (it is usually performed by considering triangular or pentagonal geometries with a radius of 1 to 5m).

Thanks to the active data recorded by a (single) 3-component geophone, we then also introduce the group-velocity spectra of both Love and Rayleigh (vertical and radial components) waves, together with the *Radial-to-Vertical Spectral Ratio* (RVSR) and the *Rayleigh-wave Particle Motion* (RPM) frequency curve.

This way we can define up to seven objective functions to jointly invert in order to obtain a well-constrained subsurface model free from significant ambiguities (non-uniqueness of the solution).

It is noteworthy to point out that all the presented methodologies require a limited field effort and an extremely-light (but properly-designed) equipment.

Introduction

The acquisition of seismic data in urban or so-to-speak extreme areas often represents a serious challenge because of a series of formidable problems related to the lack of suitable room, the background noise and several possible logistic problems that impose efficient acquisition strategies.
In addition to this, the inevitable ambiguity which is associated to the analyses performed according to a single method also imposes a multi-component approach capable of providing a sufficiently-robust subsurface model.
In the present work we briefly illustrate a series of methodologies that, thanks to the limited field effort and light equipment, can be adopted to cope with all the practical problems to face during this sort of acquisition campaigns.
In addition to the very classical HVSR (*Horizontal-to-Vertical Spectral Ratio*) curve, we will consider the Rayleigh-wave dispersion which is possibly depicted through the analysis of the *Miniature Array Analysis of Microtremors* (MAAM) as proposed by Cho *et al*. (2013). Furthermore we will also introduce the analysis of the group-velocity spectra, the *Radial-to-Vertical Spectral Ratio* (RVSR) and the effective *Rayleigh-wave Particle Motion* (RPM) frequency curve which are possible while considering the holistic analysis of the active data recorded by a single 3-component (3C) geophone (Dal Moro *et al*., 2015; 2016a; 2016b).
It is noteworthy that to acquire the data for all these techniques, are necessary only three vertical and one 3C geophones, combined and managed through a properly-designed acquisition system.

Four Geophones, Three Methods and Seven Objective Functions

The overall proposed approach aims at jointly exploiting a series of active and passive methodologies here briefly summarized:
    1) the *Horizontal-to-Vertical Spectral Ratio* [passive];
    2) the *Miniature Array Analysis of Microtremors* (MAAM) [passive - Cho *et al*. (2013)];
    3) the Holistic analysis of Surface waves (HS) [active - Dal Moro *et al*. (2015; 2016a; 2016b)].

From the first and second methods we can determine two objective functions to use during our data analysis and inversion: the HVSR curve and the dispersion curve of the Rayleigh-wave vertical-component.
From the data acquisition point of view, while for the HVSR it is necessary only one calibrated 3C geophone, for the MAAM at least 4 vertical geophones are required (please notice that, compared to other passive array techniques, the MAAM requires a significantly smaller radius - see Cho *et al*. 2013; Dal Moro *et al*., 2015). By adopting the optimized acquisition procedure described in Dal Moro *et al*. (2015) and summarized in Figure 1, we can actually efficiently jointly acquire the data for both the HVSR and MAAM methodologies.
Five more objective functions can be then determined from the HS active approach. In this case, data acquisition is accomplished by setting a single 3C geophone at a fixed distance (*offset*) from the source, and the acquisition is performed by applying both a Vertical Force (VF) [aimed at producing Rayleigh waves], both a Horizontal Force (HF) [aimed at producing Love waves - for this purpose a common wooden beam is usually adopted - for details see Dal Moro, 2014].
This way, the three acquired traces represent the Rayleigh-wave vertical and radial components and the Love waves (transversal trace).
From these (active) data is then possible to determine up to five objective functions (see Figure 2):
  1) the group-velocity spectrum of the vertical (Z) component of Rayleigh waves;
  2) the group-velocity spectrum of the radial (R) component of Rayleigh waves;
  3) the group-velocity spectrum of Love waves (T trace);
  4) the *Radial-to-Vertical Spectral Ratio* (RVSR);
  5) the RPM frequency curve (describing the actual Rayleigh-wave retrograde/prograde motion).

The computed group-velocity spectra are analyzed according to the *Full Velocity Spectrum* (FVS) approach presented in Dal Moro (2014) and used also for instance in Dal Moro *et al*. (2015).
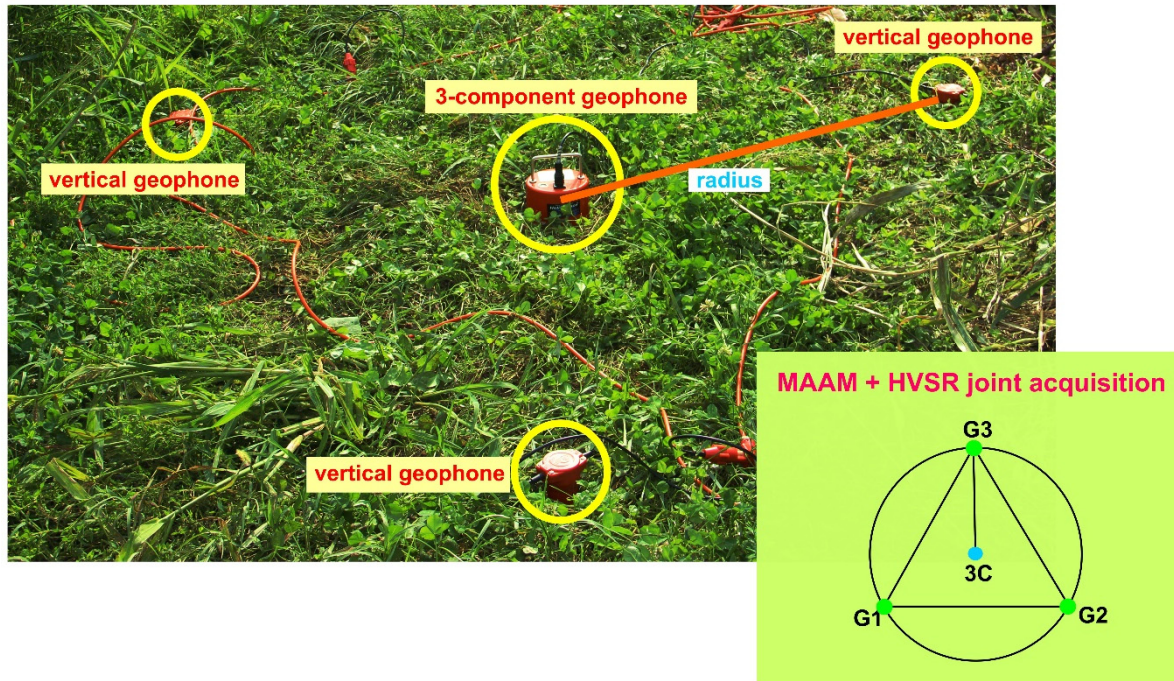
Figure 1 *Joint data acquisition for the Miniature Array Analysis of Microtremors and the H/V spectral ratio: three vertical geophones are deployed at the vertices of a triangle, while a 3-component geophone is placed at the centre.*
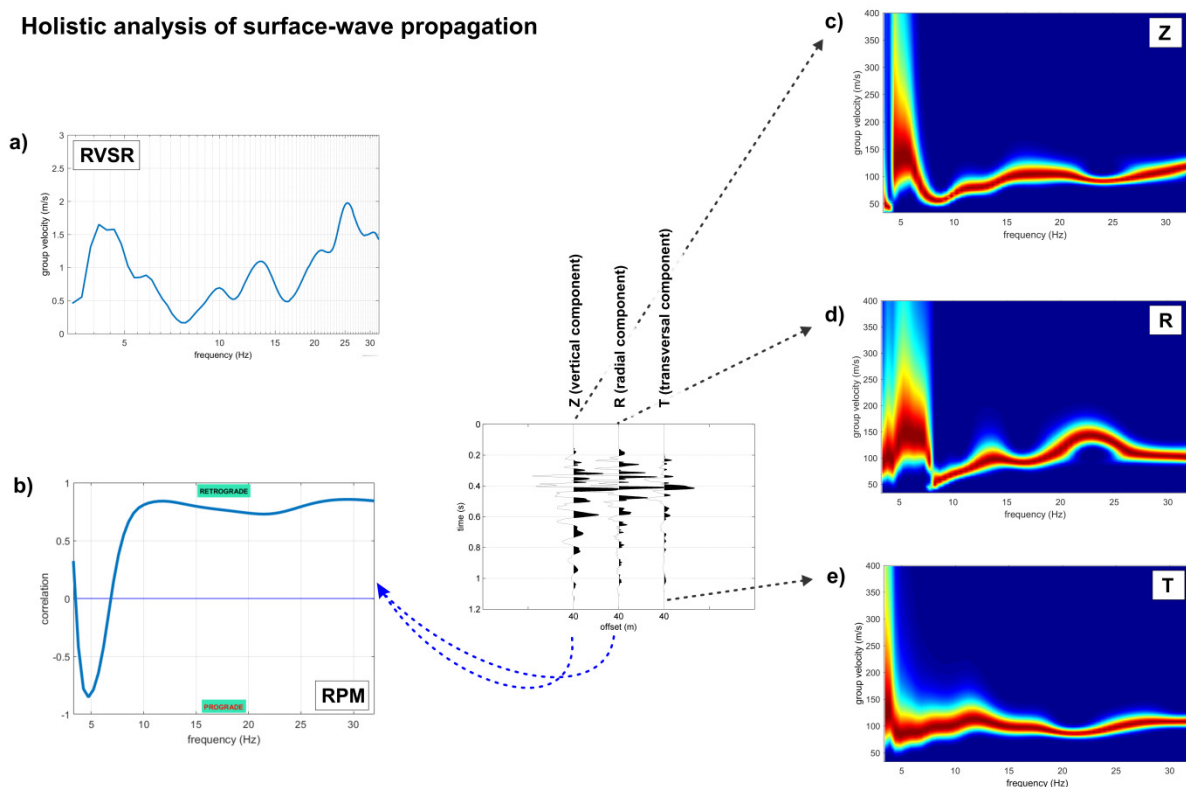

Figure 2 *Holistic analysis of the surface waves recorded by a single 3-component geophone. From the three (active) traces reported in the centre of the figure, five "objects" are computed and jointly analyzed: a) Radial-to-Vertical Spectral Ratio (RVSR); b) Rayleigh-wave Particle Motion (RPM) frequency curve; c) group-velocity spectrum of the vertical component of Rayleigh waves; d) group-velocity spectrum of the radial component of Rayleigh waves; e) group-velocity spectrum of Love waves.*

A Case Study

Data were collected in a busy commercial and residential area of Lodi (North Italy - Figure 3) while using a specifically-designed acquisition system and four 2Hz sensors (three vertical and one 3C).
The offset adopted for the HS acquisition was fixed to 40m (larger offsets were too affected by the noise related to the heavy human and industrial activities of the area) and a common 8-kg sledgehammer was used to produce the Rayleigh (VF) and Love (HF) waves.
The joint acquisition of passive data for the HVSR and MAAM analyses was performed according to the geometry reported in Figure 4a and, analogously to the procedure adopted for instance for the Extended Spatial Auto-Correlation technique (Ohori *et al*., 2002; Dal Moro *et al*., 2016b), the *effective* dispersion curve obtained from the Miniature Array Analysis of Microtremors was then inverted according to Tokimatsu *et al*. (1992), thus without its interpretation in terms of modes.
The adopted 5m-radius allowed determining the dispersion curve from about 3 up to 13Hz. The upper limit depends on the spatial aliasing (the larger the radius, the smaller the maximum identifiable frequency), while the lower limit is the result of a complex combination of factors (adopted radius, quality of the overall equipment, amount of noise in the area and processing parameters).

Figure 3 Study area (North Italy): the large building at the centre is a shopping mall surrounded by congested roads and a parking lot.
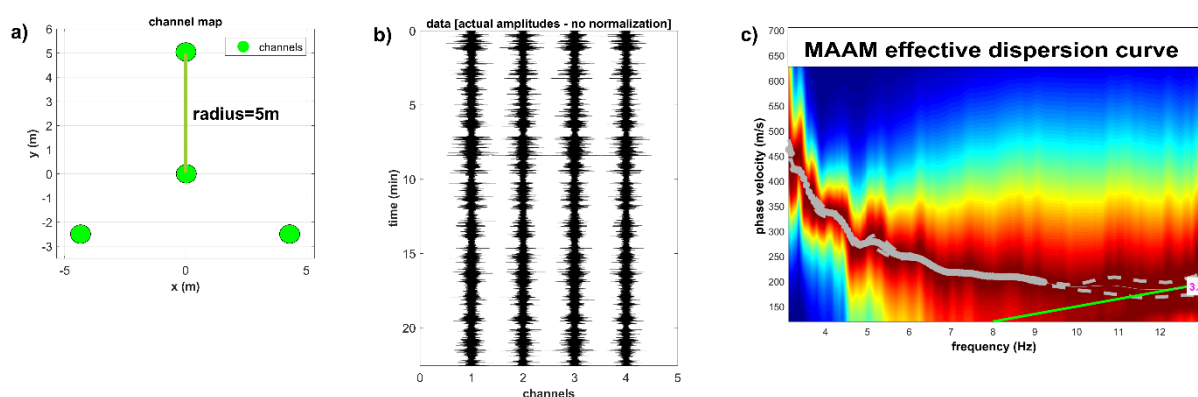

Figure 4 MAAM: a) acquisition geometry (radius 5m); b) the four 23-minute (vertical) traces; c) the obtained effective Rayleigh-wave dispersion curve (the green line report the spatial aliasing limit).

Figure 5 summarizes the results of the joint inversion for some of the considered objective functions: the two Rayleigh-wave group-velocity spectra (vertical and radial components) and the HVSR curve. While the obtained overall agreement is quite apparent and consistent with the local stratigraphy (a complex alternation of clayey sands and, more in depth, gravels), it must be underlined that a careful evaluation of the data quality is necessary in order to clean the data from possible noise components.
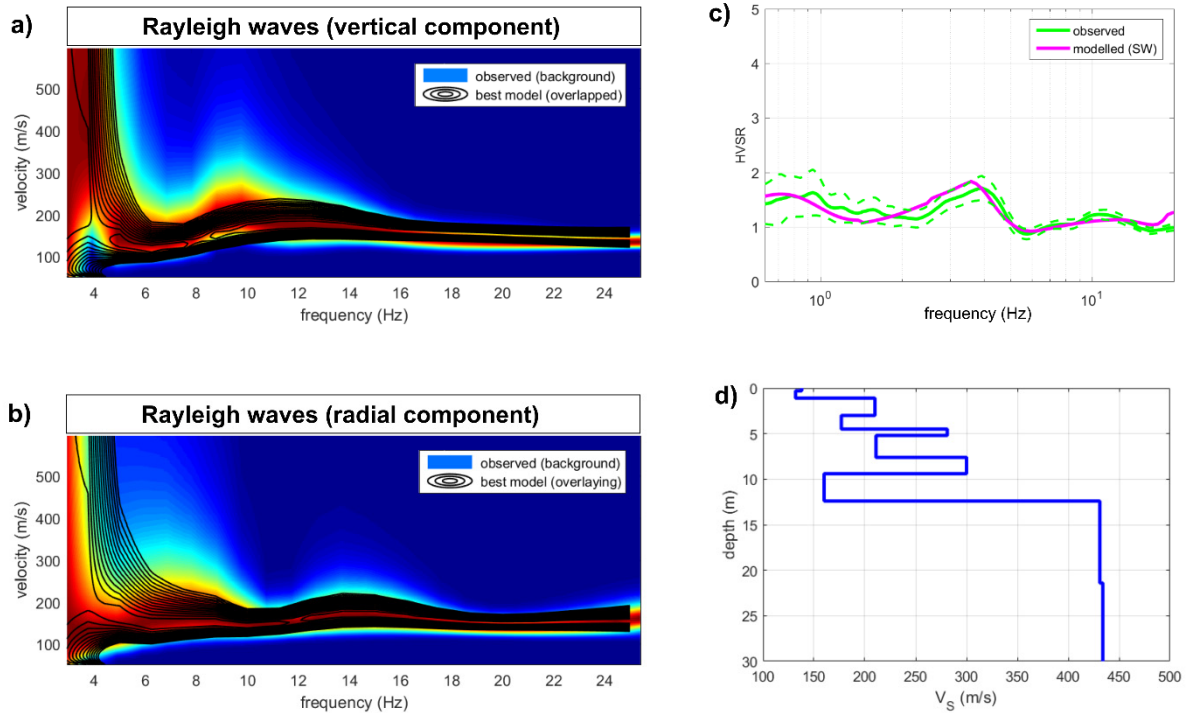
Figure 5 *Joint analysis of the group-velocity spectra of the vertical (a) and radial (b) components of Rayleigh waves (background colours represent the field data while the overlaying black contour lines the synthetic model); c) observed (green) and synthetic (magenta) HVSR; d) identified V_S model.*

Some conclusions

We briefly summarized how to possibly efficiently exploit a series of objective functions that can be determined from a mindful exploitation of a very light (but properly-designed) equipment while considering a series of active and passive methodologies that require a limited room and field effort. It must be pointed out that, although the opportunities offered by the proposed approach are quite appealing, the characteristics of these methodologies are such that, in order to properly use them, it is necessary a clear understanding of all the issues related to the role of possible noise components.

References

Cho, I., Senna, S. and Fujiwara, H. *[*2013] Miniature array analysis of microtremors. *Geophysics*, **78**, KS13–KS23.

Dal Moro, G., *Al-Arifi N.* and Moustafa S.R. *[*2016a] Analysis of Rayleigh-Wave Particle Motion from Active Seismics. Submitted to *Bull Seism. Soc. Am*.

Dal Moro, G., Moustafa, S.R. *and Al-Arifi, N. [*2016b] An efficient holistic approach to Rayleigh-wave acquisition and analysis. *Near Surface Geophysics* [accepted with minor revisions]

Dal Moro, G., Ponta, R. and Mauro R. *[*2015] Unconventional Optimized Surface Wave Acquisition and Analysis: Comparative Tests in a Perilagoon Area. *J. Appl. Geophysics*, **114**, 158-167.

Dal Moro, G. [2014] Surface Wave Analysis for Near Surface Applications. *Elsevier*, 252.

Ohori, M., Nobata, A. and Wakamatsu, K. *[*2002] A comparison of ESAC and FK methods of estimating phase velocity using arbitrarily shaped microtremor analysis. *Bull Seism. Soc. Am.*, **92**, 2323-2332.

Tokimatsu, K., Tamura, S. and Kojima, H. [1992] Effects of multiple modes on Rayleigh wave dispersion characteristics. *J. Geotech. Eng. ASCE*, **118**, 1529-1543.

Some Limitations of Geophysical Measurements in Urban Environment

C. Cornou (ISTERRE, University Grenoble Alpes/CNRS/IRD) & N. Salloum (ISTERRE, University Grenoble Alpes, Lebanese University)

Summary

Man-made artifacts (pavements, pipes) and human activities (building, mining, pumping) strongly contribute to modify near surface properties in urban sites as well as ability of geophysical methods to infer ground structure characteristics. In this paper, we illustrate some anthropic effects on various geophysical measurements performed in the city of Beirut (Lebanon).

Introduction

The shallow geology is usually characterized by considerable spatial variability in geotechnical properties, as a result of the natural processes of erosion, weathering and deposition that continuously reshape the landscape. Human activities (building, mining, pumping) have also contributed to modify near surface properties in urban sites as well as complexifying interpretation of geophysical techniques (active and passive seismics, resistivity imaging) to infer ground structure characteristics due to logistic constrain, low signal to noise ratios and man-made artifacts (concrete pipe, pollution, filling, excavation). In this paper, we illustrate some anthropic effects on geophysical measurements performed in the city of Beirut (Lebanon).

Case study

The study site is located in a flat alluvial plain in Beirut (Lebanon) which is composed of Quaternary alluvium filling that consists of interbedded layers of pebble, gravel, sand and clay overlying marly limestone of Tertiary age (Dubertret, 1944). Extensive geotechnical and geophysical measurements (active and passive surface wave measurements, single-station H/V ambient noise measurements, resistivity profiles, shear-wave downholes) have been carried out in this site (Salloum, 2015) (Figure 1). Salloum *et al*. (2014) outlined the presence over the entire area of a soft clay layer of varying thickness embedded in coarser formation (gravel, sand). During this study however, analysis and interpretation of geophysical measurements was found to be very challenging.

Indeed, the Si3 site (Figure 1) is characterized by a strong spatial superficial anthropic heterogeneity with concrete pavement remains, half-filled trenches and subsurface sewer concrete pipes. These various subsoil modifications have influenced all classical shallow geophysical measurements (active seismics, electrical profiles) as illustrated in Figure 2. Figure 2a shows two very closely located active seismic profiles: the presence of a 1.5 m diameter concrete pipe located at 1.4 m depth clearly modified Rayleigh wave propagation and related dispersion curve (Gelis *et al*., 2005). Figure 2b illustrates the effect of the discharge of pollutant substances at the surface in E3 and E4 electric images (Figure 1b), masking the bedding and the presence of the clay layer at depth.

Alternatively to classical geophysical methods, seismic ambient vibrations have been shown to be a very powerful geophysical tool in urban sites to infer ground structure properties: soil resonance frequency (e.g. Bard, 1999; Ibs-von Seht and Wohlenberg, 1999; Parolai *et al*., 2002; Haghshenas *et al*., 2008; Benjuema *et al*., 2011) and shear-wave velocity profiles (e.g. Aki, 1957; Horike, 1985; Satoh *et al*., 2001; Arai and Tokimatsu *et al*., 2004; Picozzi *et al*., 2005; Zor *et al*., 2010). In urban environments however, presence of stiff artificial material (e.g. pavement) (e.g. Castellaro and Mulgaria, 2009), sustained vibrations from machineries (e.g. SESAME, 2004) or buildings vibration (e.g. Cornou *et al*., 2004) have to be accounted for when interpreting ambient noise measurements.

For example, in Si1 site in Beirut a geotechnical company was injecting concrete for pile foundation in a 50 m deep borehole located between boreholes *B9* and *B13* during array noise measurements (Figure 1). The recorded noise (Figure 3a) is composed of numerous long transients generated by the concrete injection, as confirmed by seismic waves propagating to N40° between 4 and 10 Hz (Figure 3b). By using the simple shear-wave profile extracted at this site (Figure 3, left panel), numerical modelling of ambient noise (e.g. Bonnefoy-Claudet *et al*., 2006) generated by noise sources located at various depths in a borehole located 60 m far from the array centre has outlined that sources located in the upper sand and clay layers (i.e. source depths ranging from 1.5 to 21.5 m) excite the fundamental mode of Rayleigh wave between 2 and 10 Hz. On the opposite, noise sources located below the clay layer excite efficiently higher modes and lead to an apparent dispersion curve that is ranging between the first and the second higher modes of Rayleigh waves in the frequency band 6-10 Hz (Figure 3d), strongly suggesting that the measured dispersion curve at low frequency belongs to a higher mode of Rayleigh waves and is controlled by the noise sources depth.
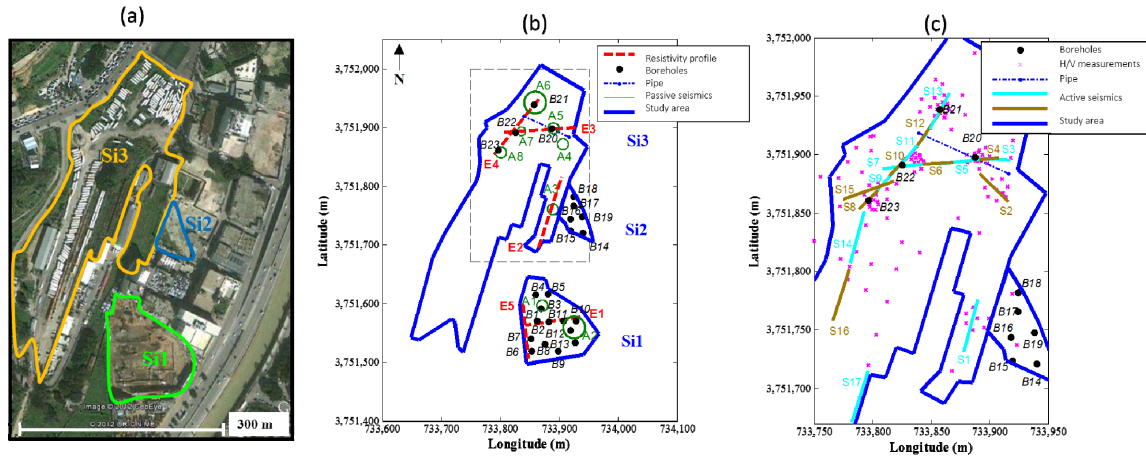
Figure 1 *(a) Location of the three study areas; (b) Location of the geotechnical (boreholes) and geophysical tests (resistivity profiles, passive seismic arrays) ; (c) Location of the geotechnical and geophysical measurements (single-station ambient noise measurements, active seismics) at Si1 site. Coordinates are in Universal Transverse Mercator (UTM). Modified from Salloum (2015).*
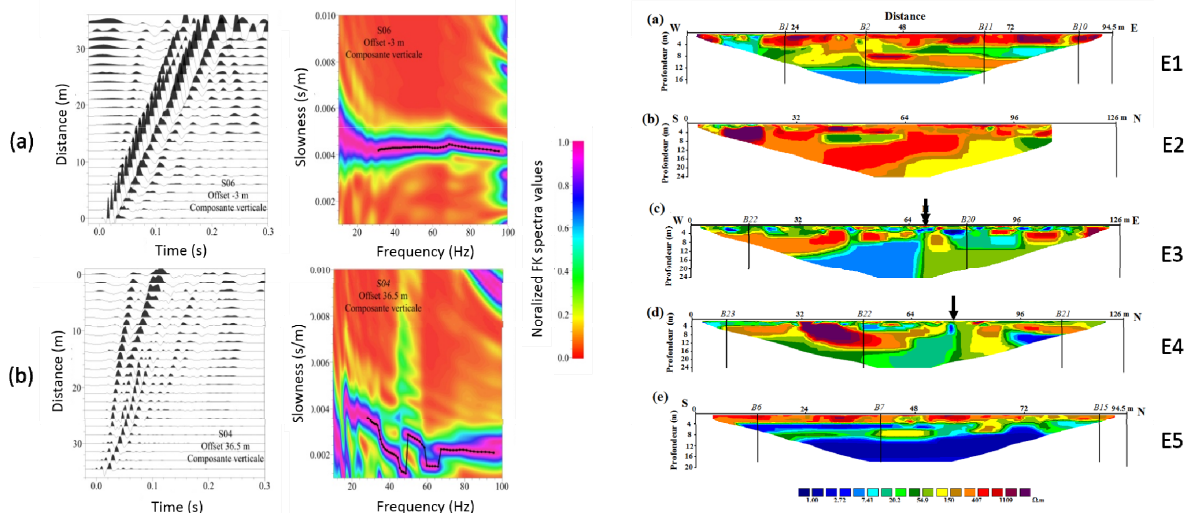

Figure 2 *(left panel) Seismic velocities (vertical component) recorded at S06 and S04 profiles (Figure 1c) and corresponding dispersion curves; (right panel) resistivity tomography at the 6 profiles indicated in Figure 1b. Location of pollution sources along E3 and E4 profiles are indicated by a black arrow. Extracted from Salloum (2015)*

Conclusions

Geophysical measurements, especially ambient noise based methods, are very appealing in urban areas and may be very efficient. However, human activities and man-made surficial heterogeneities may lead to erroneous interpretation of geophysical measurements. In such a case, careful interpretation of various investigation methods are often required to get reliable ground structure model.
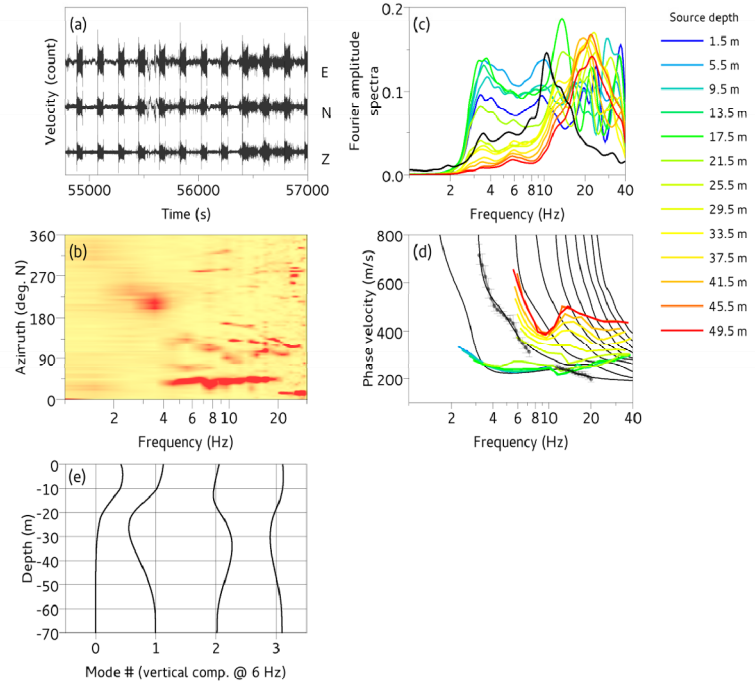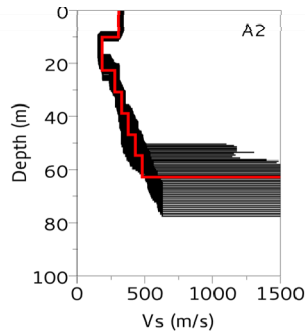
Figure 3 *(left panel) Shear-wave ensemble velocity profiles extracted at Si1 site and picture of the site; (right panel) (a) Ambient noise signals recorded at the array center; (b) Histogram of azimuths of ambient noise waves as a function of frequency. The reddest color indicates highest value of the probability density function.; (c) Fourier amplitude spectra of the noise synthetics computed at various source depths (colored lines) and of the measured noise (black line), at the array center. (d) Rayleigh wave dispersion curves derived from noise synthetics for different source depths (colored lines) and theoretical dispersion curves (black lines, first 10 modes) for the ground model shown in red in left panel. The black dots indicate the measured dispersion curve; (e) Rayleigh eigen functions for the vertical component at 6 Hz. Extracted from Salloum et al. (2014).*

References

Aki, K. [1957] Space and time spectra of stationary stochastic waves, with special reference to microtremors, *Bull. Earthq. Res. Inst.*, **35**, 415-456.

Arai, H. and Tokimatsu K. [2004] S-wave velocity profiling by inversion of microtremor H/V spectrum. *Bulletin of the Seismological Society of America*, **94**(1), 53-63.

Bard, P.-Y. [1999] Microtremor measurements: A tool for site effect estimation? Proceedings, *2nd International Symposium on the Effects of Surface Geology on Seismic Motion*, Yokohama, December 1998, 1251-1279.

Benjumea, B., Macau, A., Gabas, A., Bellmuntm, F., Figueras, S., and Cires, J. [2011] Integrated geophysical profiles and H/V microtremor measurements for subsoil characterization. *Near Surface Geophysics*, **9**(5), 413-425.

Bonnefoy-Claudet, S., Cornou, C., Bard P.Y., Cotton, F., Moczo, P., Kristek, J. and Fäh, D. [2006] H/V ratio : a tool for site effects evaluation. Results from 1D noise simulations. *Geoph. J. International*, **167**(2), 827-837.

Castellaro, S. and Mulargia, F. [2009] The effect of velocity inversions on H/V. *Pure Appl. Geophys.*, **166**, 567-92.

Cornou C., Guéguen, P., Bard, P.-Y., and Hagshenas, E. [2004] Ambient noise energy bursts observation and modeling: trapping of structure-soil harmonic induced-waves in a topmost sedimentary layer. *Journal of Seismology*, **8**(4), 507-524.

Dubertret, L. [1944] Map of Beirut and Surroundings, Edition June 1944.

Gelis, C., Leparoux, J., Virieux, J., Bitri, A., Operto, S., and Grandjean, G. [2005]. Numerical Modeling of Surface Waves Over Shallow Cavities. *J. of Env. and Eng. Geophysics,* **10**(2), 111-121.

Haghshenas, E., Bard, P.-Y., Theodulidis, N. and SESAME WP04 team [2008]. Empirical evaluation of microtremor H/V spectral ratio. *Bull Earthquake Eng*, **6**, 75-108.

Horike, M. [1985] Inversion of phase velocity of long-period microtremors to the S-wave-velocity structure down to the basement in urbanized areas. *Journal of Physics of the Earth*, **33**(2), 59-96.

Ibs-von Seht, M. and Wohlenberg J. [1999]. Microtremor measurements used to map thickness of soft sediments. *Bulletin of the Seismological Society of America*, **89**(1), 250-259.

Parolai, S., Bormann, P. and Milkereit, C. [2002] New relationships between Vs, thickness of sediments, and resonance frequency calculated by the H/V ratio of seismic noise for the Cologne area (Germany). *Bulletin of the Seismological Society of America*, **92**(6), 2521-2527.

Picozzi, M., Parolai, S. and Richwalski, S.M. [2005] Joint inversion of H/V ratios and dispersion curves from seismic noise : Estimating the S-wave velocity of bedrock. *Geophysical Research Letters*, **32**(11).

Salloum, N. [2015] *Evaluation de la variabilité spatiale des paramètres géotechniques du sol à partir de mesures géophysiques: application à la plaine alluviale de Nahr-Beyrouth (Liban).* PhD dissertation, Université Grenoble Alpes, 308.

Salloum, N., Jongmans, D., Cornou, C., Youssef Abdel Massih, D., Hage Chehade, F., Voisin, C., and Mariscal, A. [2014] The shear wave velocity structure of the heterogeneous alluvial plain of Beirut (Lebanon) : combined analysis of geophysical and geotechnical data. *Geophysical Journal International,* **199**(2), 894-913.

SESAME [2004] *Guidelines for the implementation of the H/V spectral ratio technique on ambient vibrations: Measurements, processing, and interpretation.* SESAME European research project, WP12 – Deliverable D23.12

Satoh, T., Kawase, H. and Matsushima, S. [2001] Estimation of S-wave velocity structures in and around the Sendai Basin, Japan, using array records of microtremors. *Bulletin of the seismological society of America*, **91**(2), 206-218.

Zor, E., Özalaybey, S., Karaaslan, A., Tapırdamaz, M. C., Özalaybey, S.C., Tarancıoglu, A. and Erkan, M. [2010] Shear wave velocity structure of the Izmit Bay area (Turkey) estimated from active–passive array surface wave and single-station microtremor methods. *Geoph. J. International*, **182**(3), 1603-1618.

Seismic Oicrozonation of El Ejido Vown (SE Spain) from Cmbient Poise Oeasurements

H." Seivane-Ramos (Universidad de Almería), A. García-Jerez (Universidad de Almería), M."
Navarro (Universidad de Almería), J. Piña-Flores (Instituto de Ingeniería, Universidad"
Nacional Autónoma de México), C. Aranda (Instituto Andaluz de Geofísica), F. Luzón"
(Universidad de Almería), F. Vidal (Instituto Andaluz de Geofísica) & A. Posadas (Universidad"de
Almería)*

Summary

A seismic microzonation map for El Ejido urban area, in terms of predominant periods, has
been made using ambient noise observations. Microtremor measurements were carried out at 98 sites
in this area. The predominant periods of the ground were determined from the horizontal-to-vertical
(H/V) spectral ratio technique. Moreover, portable seismic arrays were performed at two sites to get
the shear wave velocity (Vs) profiles employing the spatial autocorrelation method (SPAC) via
application of an inversion algorithm. The Vs profiles reached a depth of 40 m supporting the
classification of the soil as soft rock. Furthermore, by means of innovative software, deeper local
S-wave velocity structures have been inverted from the experimental H/V curves for one subset of
the surveyed points. All studied points in the area were found to have long natural periods ranging
from 0.8 to 2.3 s. These results suggest that the predominant peaks of low frequency observed in
H/V ratios are related to the impedance contrast between the entire column of sediments, whose
thickness varies from 200 m in the north area to 600 m in the south area of the town, and the basin
bedrock.

Introduction

Local ground conditions are relevant characteristics of the subsoil that modify the incoming seismic waves during an earthquake. Consequently, evaluation of subsurface geological conditions is a key part of seismic risk prevention in urban areas. This is the main purpose of the microtremor survey performed in El Ejido town, by means of which we have determined predominant periods and shear wave velocities, using two well known techniques of seismic noise analysis: the horizontal-to-vertical (H/V) spectral ratio (Nakamura, 1989) and the spatial autocorrelation method (Aki, 1957), respectively.

Geology and Seismicity of El Ejido town

The studied area is located in a coastal plain of SE Spain known as Campo de Dalías, being the Alboran Sea its south border and the Gádor Mountains its north border. This sedimentary basin of Quaternary and Neogene age is characterized by a metamorphic basement on which detrital materials such as gravels, sands, silts and clays have been deposited forming the Quaternary deposits and conglomeratic rocks. The Pliocene deposits are made up of calcarenites, calcirudites and finer-grained materials like clays or silts. As for the thickness of these Quaternary and Neogene sediments, it goes from 200 m on the northwestern part of the town to 600 m on the southeastern part, as presented in consulted geological references (e.g. Marín Lechado, 2005).

Several surrounding towns have been seriously affected in the last centuries by strong earthquakes (Vidal, 1986) although there are no historical reports for El Ejido town because of the fact that it has been settled as a town just few decades ago. Analysis of the two longest faults near El Ejido, Balanegra Fault (Marín Lechado *et al.*, 2010) and Loma del Viento Fault (Pedrera *et al.*, 2012), shows a possible sismogenic behaviour which would be capable of producing earthquakes from medium to high magnitudes.

Microtremor survey and data analysis

The urban area was gridded by 250 x 250 m cells, having 81 recording points into the main urban area and 19 extra points at the outskirts. In addition to these measurements, we deployed seismic pentagon shaped arrays at two available open places in this town. The acquisition equipment employed for every one of the 98 points was a Güralp CMG-6TD triaxial broadband seismometer with a sampling frequency of 100 Hz. The records were 20 minutes long.

Pentagonal arrays were deployed with several radii, from 5 to 40 m, using a portable monitoring equipment: an SPC-51A digitizer combined with six VSE-15D servo velocimeters, one per each pentagon vertex and another for the centre, both manufactured by Tokyo Sokushin Corporation. A sampling frequency of 100 Hz and a length of 30 minutes were chosen for each recorded radius.

The H/V spectra were obtained for each observation site and the predominant period of ground motion was determined using the open source software Geopsy (http://www.geopsy.org/). The signal analysis was performed windowing the records with a length of 40 s and 50% overlapping. Besides calculating H/V curves, we have inverted them. For this purpose we used a new computer code that uses the diffuse field assumption for forward modelling of the spectral ratios together with several inversion algorithms (García-Jerez et al., 2016).

The software for SPAC array processing was designed by the group of Applied Geophysics of the University of Almería. In this case, the signals were windowed with a length of 20 s and 80% overlapping.

Finally, the spatial variability of predominant periods has been analyzed through geostatistical tools. In particular, we have examined their variograms using Surfer software as a first assessment so as to seek directional trends.

Results

The analysis of our microtremor measurements shows that sites located on the NW outskirts of El Ejido have the shortest predominant periods of the dataset, between 0.7 and 1 s, meanwhile the longest periods up to 2.8 s are found mainly at the southernmost points (Figure 1). In sum, measurements into the urban area have considerably long predominant periods, ranging from 1 s on the north area to 2.3 s on the southeastern area.
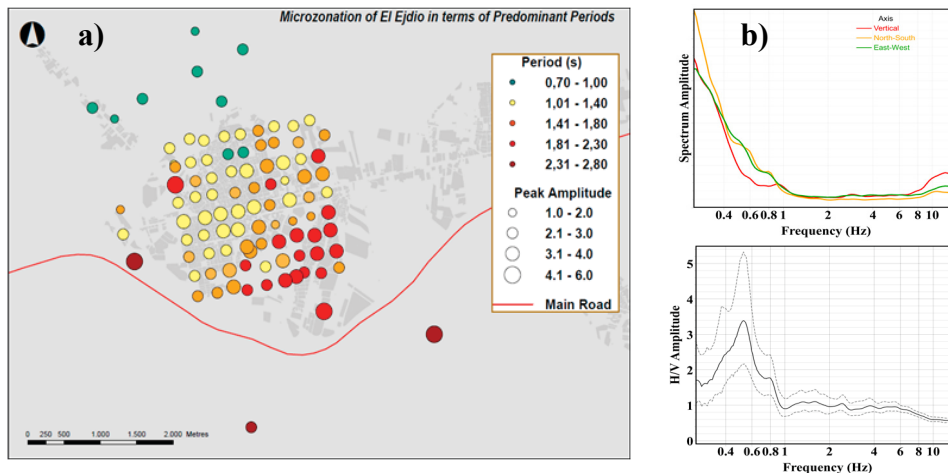

Figure 1 a) Microzonation map of El Ejido town based on the variation of the predominant period. b) Example of the amplitude spectrum and its corresponding H/V for one of the measurement points.

Variograms (Figure 2) are often direction dependent since geological characteristics are direction dependent. In this case, we know that the resonance periods are associated to sedimentary layers which show large impedance contrast with the underlying materials, so their space variability is related to the variability in thickness of those layers.
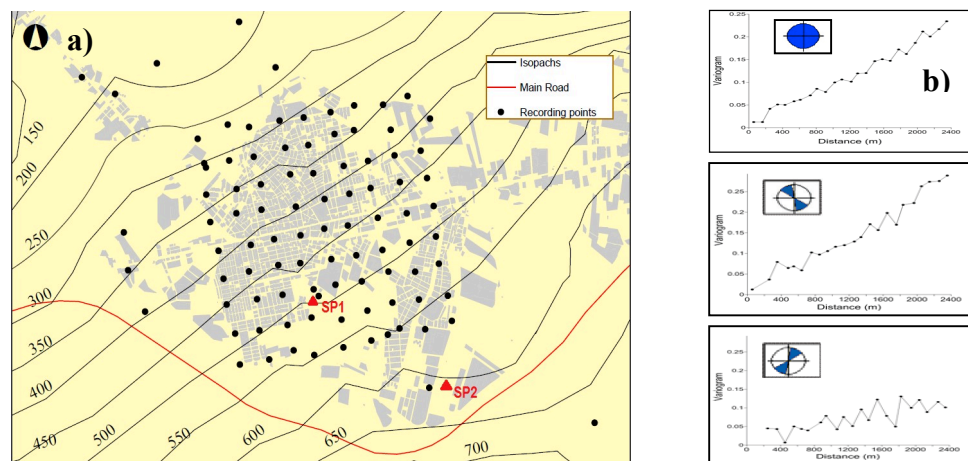

Figure 2 a) Map of microtremor recording points (SP1 and SP2 indicate places of array deployments) combined with isopachs map (thickness in metres) modified from (Marín Lechado, 2005) where the distribution of Neogene and Quaternary sediments into El Ejido urban area is showed b) Experimental directional variograms of predominant periods.

Velocity profiles (Figure 3) obtained from the SPAC method give estimated values of V_s^{30} greater than 400 m/s, so the soil could be classified according to the Spanish seismic code NCSE-02 as soft rock. This result agrees with the studied geotechnical surveys which often show Pliocene calcarenites at the top of the stratigraphic columns.
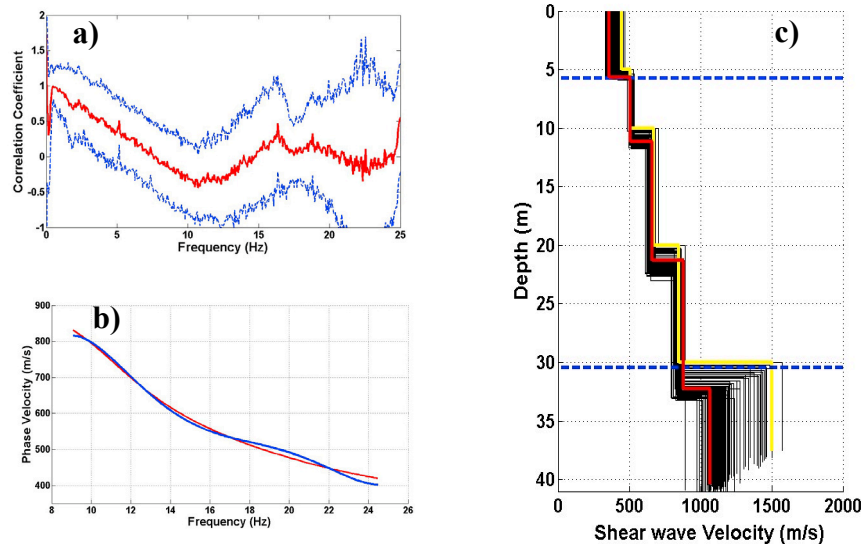

Figure 3 Example of the three followed steps during the processing of SPAC measurements at a surveyed point (SP1). a) Correlation coefficient (red) for the radius of 40 m. b) Theoretical (red) and observed (blue) dispersion curves. c) Shear wave velocity profile. Yellow line represents the initial starting model and red line the final model.

A deeper model (Figure 4) for the surveyed point analyzed in Figure 3 has been obtained inverting the H/V curve of this point. We used the HV-Inv computational code (García-Jerez *et al.*, 2016) .
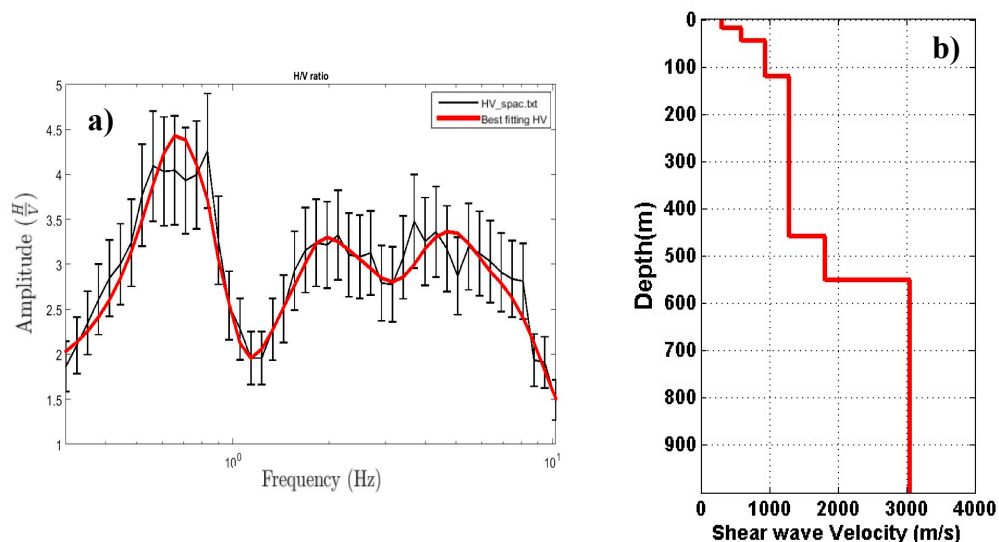

Figure 4 a) Experimental H/V curve (black line) and theoretical H/V curve for the inverted model (red line) b) Inverted Shear wave velocity profile.

Conclusions

The predominant periods were obtained using the H/V method and the study showed that predominant periods vary from 1.1 s at the north boundary of the city to 2.3 s at the southeastern part of the experimental grid covered by this study.

Isopachs of Neogene and Quaternary sediments indicate a maximum thickness variation along the NW-SE direction. So, if we study the directional variograms, for example, onto NE-SW directions, we will choose pairs of periods separated the same distance and located on nearby isopachs which leads to low semivariances (Figure 2).

Shear wave profiles extracted from the application of the SPAC method confirm the overall stiffness of soils at El Ejido urban area. The Vs^{30} values that we found were 579 m/s at the point SP1 and 646 m/s at the point SP2.

A new method based on diffuse-field theory has been successfully used for inversion of velocity models from H/V curves. This new technique allows us to investigate deep velocity contrasts linked to the long predominant periods found in El Ejido town.

Acknowledgements

References

Aki, Keiiti [1957] Space and time spectra of stochastic waves, with special reference to microtremors. Bull. Earthq. Res. Inst., 22 35, 415–456.

García-Jerez, A., Piña-Flores, J., Sánchez-Sesma, F.J., Luzón, F., Perton, M. [2016] A computer code for forward calculation and inversion of the H/V spectral ratio under the diffuse field assumption. Computers & Geosciences, Accepted. ArXiv160406406 Phys., http://www.ual.es/GruposInv/hv-inv

Marín Lechado, C. [2005] Estructura y evolución tectónica reciente del Campo de Dalías y de Níjar en el contexto del límite meridional de las Cordilleras Béticas orientales: tesis doctoral. Editorial Universidad de Granada, Granada.

Marín Lechado, C., Galindo-Zaldívar, J., Gil, A.J., Borque, M.J., de Lacy, M.C., Pedrera, A., López-Garrido, A.C., Alfaro, P., García-Tortosa, F., Ramos, M.I., Rodríguez-Caderot, G., Rodríguez-Fernández, J., Ruiz-Constán, A., de Galdeano-Equiza, C.S. [2010] Levelling Profiles and a GPS Network to Monitor the Active Folding and Faulting Deformation in the Campo de Dalias (Betic Cordillera, Southeastern Spain). Sensors 10, 3504–3518.

Nakamura, Y. [1989] A method for Dynamic Characteristics Estimation of Subsurface Using Microtremor on the Ground Surface. QR of RTRI 30, 25–33.

Pedrera, A., Marín-Lechado, C., Stich, D., Ruiz-Constán, A., Galindo-Zaldívar, J., Rey-Moral, C., de Lis Mancilla, F. [2012] Nucleation, linkage and active propagation of a segmented Quaternary normal-dextral fault: the Loma del Viento fault (Campo de Dalías, Eastern Betic Cordillera, SE Spain). Tectonophysics 522–523, 208–217.

Vidal, F. [1986] Sismotectónica de la región Beticas-Mar de Alborán. Servicio de Publicaciones, Universidad de Granada, Granada.

Seismic Interferometry for Near-surface Applications

E. Galetti* (University of Edinburgh) & A. Curtis (University of Edinburgh)

Summary

Seismic records contain information that allows geoscientists to make inferences about the structure and properties of the Earth's interior. Traditionally, seismic imaging and tomography methods require wave-fields to be generated and recorded by identifiable sources and receivers, and use these directly-recorded signals to create models of the Earth's subsurface. However, in recent years the method of seismic in-terferometry has revolutionised earthquake seismology by allowing unrecorded signals between pairs of receivers, pairs of sources, and source-receiver pairs to be constructed as Green's functions using either cross-correlation, convolution or deconvolution of wavefields. In all of these formulations, seis-mic energy is recorded and emitted by surrounding boundaries of receivers and sources, which need not be active and impulsive but may even constitute continuous, naturally-occurring seismic ambient noise. Within this paper, we will review the theory of seismic interferometry, present examples of its use in both crustal and exploration seismology settings, and explore its potential for smaller-scale applications.

Introduction

Just as X-rays are commonly used in medicine to study the human body, seismic waves are used in geophysics to study the interior of the Earth. Seismic waves are generated within and on the Earth's surface by impulsive or finite sources of energy of either natural or man-made origin. These waves travel through the Earth's subsurface, are transmitted, reflected, diffracted and refracted by inhomogeneities in the different materials that they encounter, and cause the particles of the medium of propagation to vibrate as they pass. Such vibrations are generally referred to as the *medium response*, and they can be recorded using seismic sensors located either beneath or on the Earth's surface. These sensors may measure ground displacement, velocity or particle acceleration with time, and seismologists can analyse the recorded medium responses to infer the properties and structure of the portion of Earth through which the waves have propagated.

Traditionally, seismologists in both academia and industry study the Earth's interior by analysing source-to-receiver records obtained from active energy sources, such as earthquakes or explosions. However, over the last decade, the field of seismology has been revolutionised by the advent and development of a new method known as *seismic interferometry*. Contrary to traditional seismology, which uses the directly-recorded medium response to deduce the properties of the Earth's subsurface, seismic interferometry can be used to construct previously unrecorded Green's functions (i.e., impulse responses) by applying either cross-correlation, convolution or deconvolution to recorded wavefields. Through this method, a *virtual seismic source* can be created at the location of any real seismic receiver (inter-receiver interferometry – see e.g. Wapenaar and Fokkema (2006) and van Manen *et al.* (2005)) and a *virtual seismic receiver* can be placed at the location of any real seismic source (inter-source interferometry – see e.g. Curtis *et al.* (2009)), where the word *virtual* is used in the sense of *imagined* (as in virtual reality). This is done using boundaries of seismic sources or receivers which surround the real receiver or source, respectively. Using a combination of source and receiver boundaries, a previously unrecorded Green's function can also be constructed between a *virtual source* and a *virtual receiver* (source-receiver interferometry – Curtis and Halliday (2010)). In addition, seismic sources on the surrounding boundaries need not be active or impulsive (i.e., earthquakes in crustal seismology, dynamite or vibroseis in exploration seismology) but may be of passive origin (i.e., wind, oceanic waves, microseismic and anthropogenic activity). In fact, seismic waves generated by passive noise sources travel through the Earth's interior just like those that originate from active sources and, because such noise sources are widespread, may even sample areas that are not usually probed by waves of active origin.

Hence, thanks to seismic interferometry, what was previously referred to as contaminating 'noise' and was commonly removed from recorded datasets to enhance the quality of coherent signals, can now be decoded to extract useful information on the Earth's subsurface by creating new, artificial seismograms. Such seismograms can then be treated just like active-source records to image the real Earth's interior using more or less traditional imaging methods.

Background to the theory of seismic interferometry

Classical inter-receiver interferometry by cross-correlation uses a boundary of seismic sources to construct the wavefield that would propagate between the locations of two receivers within the medium of propagation (Figure 1). The traces recorded at the two receivers from each source on the boundary are first cross-correlated, and all cross-correlations are then stacked (summed) over the source positions. The result is a two-sided signal, where each side represents energy travelling between the two receivers in one or other of the opposite directions. In mathematical form, this process can be represented by the following formula given in the frequency domain (Wapenaar and Fokkema, 2006):

$$G(\mathbf{x}_B, \mathbf{x}_A) - G^*(\mathbf{x}_B, \mathbf{x}_A) = \int_S \frac{1}{\rho(\mathbf{x})} \left[(\partial_j G(\mathbf{x}_B, \mathbf{x})) G^*(\mathbf{x}_A, \mathbf{x}) - G(\mathbf{x}_B, \mathbf{x}) (\partial_j G^*(\mathbf{x}_A, \mathbf{x})) \right] n_j \, \mathrm{d}S. \quad (1)$$

Here, the asterisk * denotes complex conjugation (i.e., cross-correlation in the frequency domain corresponds to a product when the complex conjugate of one of the factors is taken first), $\rho(\mathbf{x})$ is the density
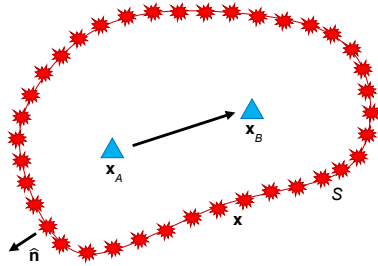
Figure 1 *Schematic illustration of a typical geometry for cross-correlational seismic interferometry. Two receivers (blue triangles) are surrounded by a boundary of sources (red explosions). At each source position, the boundary normal is denoted by* n̂. *Seismic interferometry turns one of the receivers (e.g.,* $\mathbf{x}_A$*) into a virtual source, and constructs the Green's function as though this source was recorded by the other receiver (e.g.,* $\mathbf{x}_B$*).*

of the medium at $\mathbf{x}$, ∂_j represents partial differentiation in the x_j-direction with respect to the source coordinate $\mathbf{x}$, n_j is the component of the boundary normal along the x_j-direction, and G and $\partial_j G$ represent Green's functions as responses to monopole and dipole sources. By assuming a high frequency regime, that the surrounding surface of sources S is a sphere with very large radius, and that no energy scatters back through S once it has left, equation (1) can be simplified using the Sommerfield radiation conditions to eliminate the derivatives, giving (Wapenaar and Fokkema, 2006):

$$G(\mathbf{x}_B, \mathbf{x}_A) - G^*(\mathbf{x}_B, \mathbf{x}_A) \approx -\frac{2\iota\omega}{\rho c} \int_S G(\mathbf{x}_B, \mathbf{x}) G^*(\mathbf{x}_A, \mathbf{x}) \, \mathrm{d}S, \qquad (2)$$

where c is the propagation velocity of the medium and ι is the imaginary unit. The result of either of equations (1) and (2) is a two sided signal, at positive and negative times: the causal (positive-time) part of the signal represents the Green's function between $\mathbf{x}_A$ and $\mathbf{x}_B$, while the acausal (negative-time) part of the signal represents the negative of the Green's function between $\mathbf{x}_A$ and $\mathbf{x}_B$.

Example 1: Ambient noise traveltime tomography

Within crustal seismology, a very common application of seismic interferometry is ambient-noise tomography (ANT). ANT is an Earth imaging method which makes use of inter-station Green's functions constructed from cross-correlation of seismic ambient noise records to image the Earth's subsurface tomographically. It is particularly useful in seismically quiescent areas where traditional tomography methods that rely on local earthquake sources would fail to produce interpretable results due to the lack of available data. Once constructed, interferometric Green's functions can be analysed using standard waveform analysis techniques, and inverted for subsurface structure using more or less traditional imaging methods.

Figure 2 shows results of ambient noise tomography at 10 seconds period for the British Isles, which are characterised by low levels of earthquake activity and hence could not easily be imaged using surface waves from local-earthquake data. However, being an archipelago bounded by the Atlantic Ocean to the west, the North Sea to the east and the Norwegian Sea to the north, the British Isles are naturally surrounded by sources of seismic ambient noise, which constitute the boundary S shown in Figure 1. By cross-correlating ambient noise traces recorded at a number of seismic stations (white triangles in Figure 2), we constructed Green's functions for a large number of inter-station paths, and used the Love-wave traveltimes retrieved from these Green's functions to perform seismic traveltime tomography with a fully non-linear, transdimensional Monte Carlo algorithm (Galetti *et al.*, 2015).

Example 2: Ground roll estimation and removal

Within industrial exploration, surface wave retrieval from seismic interferometry has proved useful in estimating and removing ground roll (the industrial term for surface waves) from acquired reflection data. Ground roll consists of direct and scattered surface waves which propagate from the source to a receiver within the shallowest layers of the Earth, and due to its high amplitude it often masks the deeper-reflecting arrivals which are of interest in seismic exploration. In addition, scattered ground-roll may occupy the same part of frequency-wavenumber (f-k) space as the body wave reflections or refractions of interest, making it usually difficult to remove using standard f-k filters.
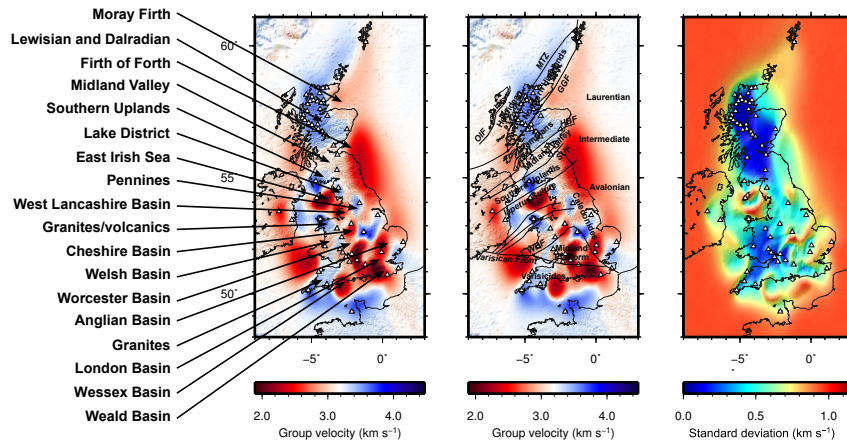
Figure 2 *Average Love-wave group velocity map of the British Isles (left and centre) and associated standard deviation (right) from fully non-linear, transdimensional Monte Carlo ambient noise tomography (Galetti et al., 2015) at 10 seconds period. The main geological structures are indicated on the left-hand map, and terrane boundaries after Woodcock and Strachan (2012) are overlaid on the central map. Seismic stations are denoted by white triangles.*
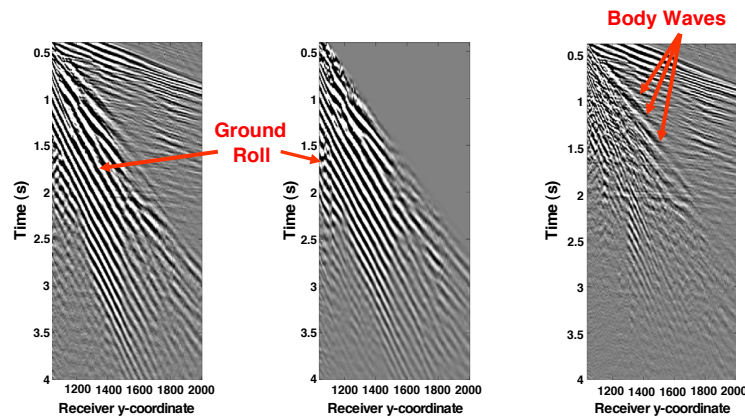

Figure 3 *Example of scattered ground roll removal through seismic interferometry. The raw data is shown on the left, and ground roll predicted from seismic interferometry is shown in the central panel. By subtracting the adaptively filtered ground roll obtained through seismic interferometry from the raw data, the cleaner data on the right is obtained. Modified after Halliday (2010).*

Figure 3 shows the application of seismic interferometry to ground roll prediction and removal as illustrated by Halliday (2010): scattered surface waves are first predicted using seismic interferometry (central panel); these signals, after being adaptively filtered, are then subtracted from the raw data on the left to give the cleaner data set on the right, where body waves are clearly visible.

Example 3: Time-dependent monitoring

Coda-wave interferometry (CWI) (Snieder *et al.*, 2002) is a subsurface monitoring technique which makes use of recordings of multiply scattered waves (i.e., the *coda* of a seismic signal) in order to infer time-dependent changes within the medium. Thanks to multiple scattering, coda waves have much longer propagation paths compared to directly arriving phases, hence they are sensitive to changes within a very large volume of the medium. Therefore, if a perturbation in the medium (i.e., a bulk variation in velocity, a change in scatterer positions, etc.) occurs over time, it can be identified by changes in the traveltimes of coda waves, while such changes are usually undetectable in the first arrivals.

Coda wave interferometry has been used for time-dependent monitoring at a variety of scales, from large-scale volcanic edifices (Grêt *et al.*, 2005) to small-scale civil engineering structures (Stähler *et al.*, 2011).
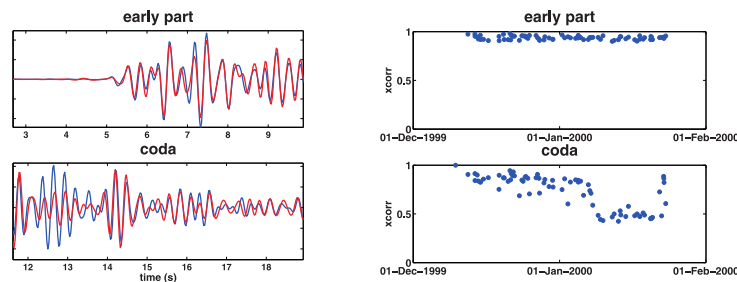
Figure 4 *Comparison of waveforms recorded at Mount Erebus volcano for two Strombolian eruptions two weeks apart in time (left), and correlation coefficients between a number of eruption seismograms and a reference trace (right) recorded during a period of strong volcanic activity. Early time segments are shown on the top; late coda segments are shown on the bottom. Modified after Grêt et al. (2005).*

An example of the former application is illustrated in Figure 4, which shows the responses recorded on Mount Erebus volcano in Antarctica due to explosive Strombolian eruptions. The two waveforms in the left column, recorded two weeks apart in time, appear to match relatively well when the early arrivals are considered (top), while the late coda waveforms (bottom) do not match and appear to be shifted in time due to changes that occurred within the interior of the volcano. This can also be observed in the correlation coefficients shown in the right column, which were calculated between a number of Strombolian eruption seismograms and a reference trace from the beginning of the monitoring period.

Conclusions

Seismic records contain information that allows geoscientists to make inferences about the properties and structure of the Earth's subsurface. Seismic interferometry allows the retrieval of useful information on the subsurface by extracting signal from what is normally considered as contaminating noise. Thanks to its applicability at a variety of scales, this technique has revolutionised seismic imaging and monitoring of the Earth's interior, and has successfully been employed in a variety of settings from from earthquake and volcano seismology to industrial exploration and civil engineering.

References

Curtis, A. and Halliday, D. [2010] Source-receiver wave field interferometry. *Physical Review E*, **81**(4), 046601.

Curtis, A., Nicolson, H., Halliday, D., Trampert, J. and Baptie, B. [2009] Virtual seismometers in the subsurface of the Earth from seismic interferometry. *Nature Geoscience*, **2**(10), 700–704.

Galetti, E., Curtis, A., Meles, G.A. and Baptie, B. [2015] Uncertainty loops in travel-time tomography from nonlinear wave physics. *Physical Review Letters*, **114**(14), 148501.

Grêt, A., Snieder, R., Aster, R.C. and Kyle, P.R. [2005] Monitoring rapid temporal change in a volcano with coda wave interferometry. *Geophysical Research Letters*, **32**(6), L06304.

Halliday, D. [2010] Adaptive model-driven interferometry for ground-roll attenuation. *SEG Technical Program Expanded Abstracts 2010*, 3550–3554.

van Manen, D.J., Robertsson, J.O.A. and Curtis, A. [2005] Modeling of Wave Propagation in Inhomogeneous Media. *Physical Review Letters*, **94**(16), 164301.

Snieder, R., Grêt, A., Douma, H. and Scales, J. [2002] Coda Wave Interferometry for Estimating Nonlinear Behavior in Seismic Velocity. *Science*, **295**(5563), 2253–2255.

Stähler, S.C., Sens-Schönfelder, C. and Niederleithinger, E. [2011] Monitoring stress changes in a concrete bridge with coda wave interferometry. *The Journal of the Acoustical Society of America*, **129**(4), 1945–1952.

Wapenaar, K. and Fokkema, J. [2006] Green's function representations for seismic interferometry. *Geophysics*, **71**(4), SI33–SI46.

Woodcock, N.H. and Strachan, R. [2012] *Geological History of Britain and Ireland.* Wiley-Blackwell, 2 edn.

Optimization of Equipment for Ambient Noise Array Measurements

*J.J. Galiana-Merino * (University of Alicante, Spain), S. Rosa-Cintas (University of Alicante, Spain), J.L. Soler-Llorens (University of Alicante, Spain), J. Rosa-Herranz (University of Alicante, Spain)*

Summary

For developing microzonation studies using ambient noise array measurements, the kind and number of available sensors play a key role in the design of the field campaign. In this work we show different strategies of how optimizing the available resources in order to implement appropriate array measurements.

First approach deals with the suitability of seismic refraction/reflection equipment of geophones to work in a frequency range much below than their own natural frequency. In a second approach we face the handicap of having a reduced number of sensors, showing two possible solutions: a) improve the array design (geometry and size) so as to extend its capability of analysis in the lower frequency range, providing dispersion curves very similar to those obtained with bigger and denser (i.e., with more stations) layouts; b) use a reduced number of M sensors to implement bigger arrays of N sensors positions (M < N), by only increasing the recording time of the M stations in different positions of the original prearranged N stations geometry. Finally, we also show the possibility of designing our own data acquisition equipment based on low-cost open-hardware systems.

The main objective of these strategies is to provide small research groups, which usually have limited resources, with tools and procedures that allow them to perform suitable ambient noise array measurements.

Introduction

In this work we show different strategies of how optimizing the available equipment (e.g. kind and number of sensors) in order to implement appropriate array measurements. First approach deals with the suitability of seismic sensors to work in a frequency range much below than their own natural frequency (e.g. Strollo *et al*., 2008a,b; Galiana-Merino *et al*., 2011; Rosa-Cintas *et al*., 2013). In a second approach we face the handicap of having a reduced number of sensors for the field campaign. Two possible solutions are presented in terms of improving the array design, so as to extend its capability of analysis in the lower frequency range (Rosa-Cintas *et al*., 2014), and of using a reduced number of stations to implement bigger arrays of more sensors positions, by only increasing the recording time of the available stations in different positions (Galiana-Merino *et al*., 2016). Finally, we also show the possibility of designing our own data acquisition equipment based on low-cost open-hardware systems (Soler-Llorens *et al*., 2016). All these strategies can be very useful for small research groups, with limited resources, so they can perform good quality array measurements.

Suitability of vertical geophones below their natural frequency

For H/V analysis, geophones of 1Hz and 4.5Hz can retrieve reliable H/V peaks for frequencies less than 0.2 and 0.6 Hz, respectively (Strollo *et al*., 2008a,b). Although these results are important, the conclusions will certainly depend on instrument sensitivity and local noise amplitudes.

In the case of array measurements and the f-k analysis, Galiana-Merino *et al*. (2011) and Rosa-Cintas *et al*. (2013) have compared the dispersion curves obtained with sensors of different characteristics. Two examples of that are shown in Figure 1: Broadband sensors and 4.5 Hz geophones at Dhanauri, India (Figure 1a); and 1 Hz sensors and 10 Hz geophones at Almoradí, Spain (Figure 1b).
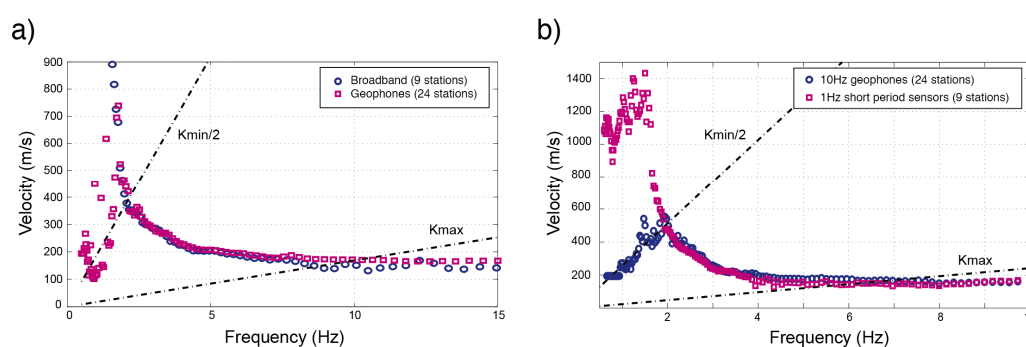

Figure 1 *Comparison of dispersion curves obtained from measurements with: a) Broadband and 4.5 Hz geophones (Dhanauri, India) and b) 1 Hz sensors and 10 Hz geophones (Almoradí, Spain)*

The obtained results show good concordance between the compared sets of stations within the theoretical wavenumber limits (kmin/2 and kmax) of the reference arrays, i.e. the broadband sensors in (a) an the 1 Hz sensors in (b). It means that the usable frequency range of the geophones dispersion curves could be extended in the lower frequencies at least to 2 Hz, in both locations of study.

Optimization of the number of sensors: Experimental outcomes for f-k analysis

Several papers study the array optimization in terms of geometry and number of stations by using the SPAC method (e.g. Claprood and Asten, 2010). Whereas, concerning the array optimization with f-k method, one can find less research in the literature (e.g. Kind *et al*.,2005).

In our studies (Rosa-Cintas *et al*., 2014) we carry out an experimental work to carefully analyze the station missing effect over different prearranged array configurations (triangular, circular with central station and polygonal geometries) and then, determine the minimum number of stations that would provide reliable dispersion curves for the analyzed arrays. In this optimization study we analyze

together the theoretical array responses and the experimental dispersion curves obtained through the f-k method. The dispersion curves evaluation is performed by comparing the ones obtained for the full stations arrays with the curves of the modified arrays, in terms of a misfit function. Figure 2 shows some examples for a 7-stations triangular geometry.
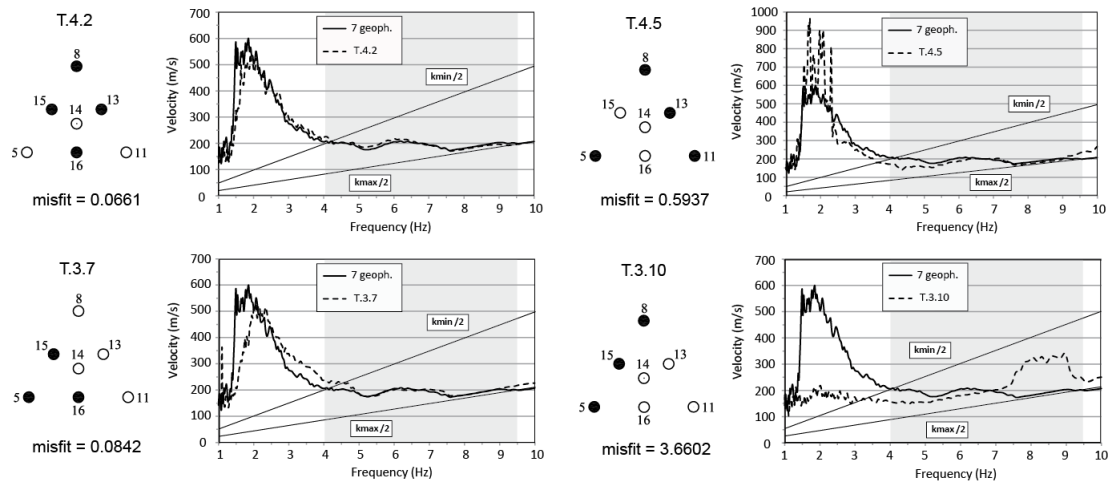

Figure 2 Comparison of dispersion curves in a 7-stations triangular array. On top row, two cases where 3 geophones have been removed are compared to the original 7-stations curve. On bottom row, two cases where 4 geophones have been removed are compared to the original one. The misfit values are shown beneath each configuration.

The displayed examples show two cases where 3 geophones have been removed on top row. The left layout is the one that provides the minimum misfit among all the tested configurations, while the right one shows the worst result. In general, when the number of usable stations is reduced, we should try to preserve the central symmetry of the theoretical array response and to position the sensors maintaining the spatial continuity among them. On bottom row, the removal of 4 sensors provides the best result with a small triangular array of 3 geophones and the worst one with a configuration where the sensors are aligned.

From the analysis carried out, it is shown that with a small-aperture, but well-configured array, it is possible to extend by far their capability of analysis in the lower frequency range, providing dispersion curves very similar to those obtained with bigger layouts. On the other hand, by separating too much the stations or lining them up, the analysis can provide very bad dispersion curves.

Use of the available sensors to the application of the ESAC method

There is another way to overcome the lack of a great number of sensors in the field experiments. The number of accessible sensors might be limited but both the recording time and the position of each sensor on the field are not. Thus, Galiana-Merino *et al*. (2016) propose a new methodology to implement an N sensors arrangement by using only M sensors (M<N), which are recording in different positions of the original predesigned N sensors geometry at different times. The complete measurements associated to the original geometry of N receiver positions is conformed of several recording sets performed by reduced groups of M sensors, placed in determined positions of the original layout, each time. The number of required measurement sets has to be enough to assure that all the pairs of sensors present in the original arrangement of N receiver positions are analyzed at least once in the complete process.

The proposed procedure has been evaluated through synthetic and real tests to demonstrate the accuracy and stability of the developed approach. Arrays with different number of stations, M, have been tested by comparing the obtained results with the expected ones, when N stations are available.

In the example shown in Figure 3, we study a circular array of 25m of aperture located in the village of Almoradi (southeast Spain) and we show the dispersion curves obtained using sets of 2, 3, 4 and 5 sensors. In all these cases, the estimated results have been compared with the one obtained by the common procedure, i.e. with the 8 sensors recording simultaneously.
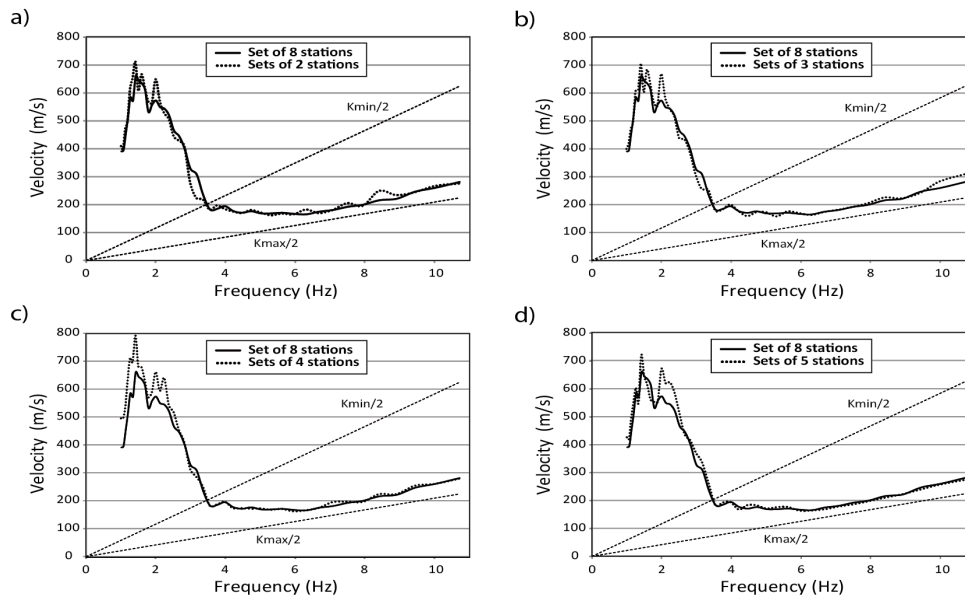

Figure 3 Mean dispersion curves obtained for sets of 2 (a), 3 (b), 4 (c) and 5 (d) sensors, together with the dispersion curve estimated using the 8 stations recording simultaneously.

This research shows the viability of using a reduced number of sensors to implement bigger and denser arrays by only increasing the total recording time and moving some of the sensors, which might be especially useful for small research groups, where the number of available sensors is limited by economic constraints.

Low-cost open-hardware data acquisition systems

The high price of the data acquisition equipment and the necessity of building custom-made experimental systems to acquire data through sensors have made that some research groups develop their own equipment, adapted to their needs (e.g. Picozzi *et al*. 2010).

In this sense, in Soler-Llorens *et al*. (2016), a low-cost Arduino-based seismic recorder for vertical geophones has been developed as starting point for future array measurements. Arduino constitutes an open-source electronic platform that allows monitoring and controlling different analog and digital signals, as well as other specific electronic circuits. The system is controlled through a user interface developed ad hoc, which includes the parameters needed for the data acquisition and recording.

The evaluation tests demonstrate the suitability of the developed system to acquire and record seismic signals, with the same reliability as other commercial equipment. Thus, it provides a low-cost alternative to the commercial systems. Moreover, this is an open-source system, which allows other users to carry out hardware and software changes, in order to adapt the proposed prototype to their particular requirements. It is appropriate for different educational and research seismic experiments, including the seismic monitoring for long periods of time (e.g. ambient noise measurements).

Conclusions

Array measurements require the use of several stations recording simultaneously. In this sense, any saving in the number of sensors and even in the equipment themselves can benefit microzonation studies in urban areas carried out by small research groups. Thus, we have studied the suitability of some

geophones to work at frequencies below its natural one, as well as different ways to reduce the number of required sensors. Currently, we are also designing and testing new low-cost acquisition systems for array measurements.

Acknowledgements

References

Strollo A., Bindi D., Parolai S., Jäckel K-H. [2008a] On the suitability of 1s geophone for ambient noise measurements in the 0.1-20 Hz frequency range: experimental outcomes. *Bull. Earthq. Eng.*, **6**, 141-147.

Strollo A., Parolai S., Jäckel K-H., Marzorati S., Bindi D. [2008b] Suitability of short-period sensors for retrieving reliable H/V peaks for frequencies less than 1 Hz. *Bull. Seismol. Soc. Am.*, **98**(2),671-681.

Galiana-Merino, J.J., Mahajan, A.K., Lindholm, C., Rosa-Herranz, J., Mundepi, A.K. and·Nitesh Rai [2011] Seismic noise array measurements using broadband stations and vertical geophones: preliminary outcomes for the suitability on f-k analysis. *Bull. Earthq. Eng.*, **9**, 1309-1325.

Rosa-Cintas, S., Galiana-Merino, J.J., Rosa-Herranz, J., Molina, S. and Giner-Caturla, J. [2013] Suitability of 10 Hz vertical geophones for seismic noise array measurements based on frequency-wavenumber and extended spatial autocorrelation analyses. *Geophys. Prospect.*, **61**, 183-198.

Rosa-Cintas, S., Galiana-Merino, J.J., Alfaro, P. and Rosa-Herranz, J. [2014] Optimizing the number of stations in arrays measurements: Experimental outcomes for different array geometries and the f–k method. *J. Appl. Geophys.*, **102**, 96-133.

Galiana-Merino, J.J., Rosa-Cintas, S., Rosa-Herranz, J., Garrido, J., Peláez, J.A., Martino S. and Delgado, J. [2016] Array measurements adapted to the number of available sensors: Theoretical and practical approach for ESAC method. *J. Appl. Geophys.*, **128**, 68-78.

Soler-Llorens, J.L., Galiana-Merino, J.J., Giner-Caturla, J., Jauregui-Eslava, P., Rosa-Cintas, S. and Rosa-Herranz, J. [2016b] Development and programming of Geophonino: A low cost Arduino-based seismic recorder for vertical geophones. *Comput. Geosci.*, **94**, 1-10.

Claprood, M., Asten, M.W. [2010] Statistical Validity Control on SPAC Microtremor Observations Recorded with a Restricted Number of Sensors. *Bull. Seismol Soc. Am.*, **100**(2), 776-791.

Kind, F., Fäh, D., Giardini, D. [2005[Array measurements of S-wave velocities from ambient vibrations. *Geophy. J. Int.*, **160**, 114-126.

Picozzi, M., Milkereit, C., Parolai, S., Jaeckel, K.H., Veit, I., Fischer, J., Zschau, J. [2010] GFZ Wireless Seismic Array (GFZ-WISE), a Wireless Mesh Network of Seismic Sensors: New Perspectives for Seismic Noise Array Investigations and Site Monitoring. *Sensors*, **10**, 3280-3304.